International Journal of
Thermofluid Science and Technology

MDPI

Review

Advances in Thermal Enhanced Oil Recovery: From Fundamental Mechanisms to Field-Scale Applications and Screening Frameworks

Abdelaziz L. Khlaifat *, Sherif Fakher, Ahmed Negm, Ahmed Einar, Amira El-Banbi, Mennatallah Gehad, Shady Shaaban and Shams ElDakar

Department of Petroleum and Energy Engineering, School of Sciences and Engineering, American University in Cairo, Cairo 11835, Egypt; sherif.fakher@aucegypt.edu (S.F.)
* Correspondence: abdelaziz.khlaifat@aucegypt.edu

Abstract

Thermal traditional enhanced oil recovery (EOR) screening has long relied on static lookup tables that filter candidate reservoirs using fixed, isolated property cutoffs such as depth, net pay, permeability, and viscosity. While useful for preliminary sorting, these static matrices fail to capture non-isothermal thermodynamics, transient geomechanical stress fields, dynamic fluid-phase behaviors, and the stringent economic and environmental constraints governing modern heavy oil assets. This manuscript introduces a dynamic, four-stage integrated decision architecture that transforms thermal EOR (TEOR) screening from a passive collection of property thresholds into an actionable, physics-governed engineering workflow. The primary novelty of this work lies in its holistic synthesis across five previously siloed operational domains: steam-solvent hybrids, late-stage SAGD with non-condensable gas (NCG) co-injection, electromagnetic/radio-frequency heating, machine learning applications, and CCUS-coupled recovery. Unlike previous reviews that analyze standalone recovery techniques or unconstrained "black-box" predictive models, this framework explicitly integrates operational boundary exceptions (for example, Vacuum Insulated Tubing, Downhole Steam Generation, and solvent prepads) that extend traditional depth, thin-pay, and tight-matrix screening limits. Furthermore, it embeds concrete, physics-informed machine learning applications—ranging from facies proxy models and spatial–temporal steam chamber predictors to dynamic Steam-Oil Ratio (SOR) optimizers and real-time failure detectors—directly into sequential screening gates. Every parameter cutoff across Cyclic Steam Stimulation, Steam-Assisted Gravity Drainage, In Situ Combustion, and Electromagnetic Heating is thoroughly justified through fluid dynamics, heat transfer thermodynamics, geomechanics, and combustion kinetics. By systematically evaluating candidate reservoirs through four sequential decision gates, Thermodynamic Viability, Container Integrity, Lifecycle Carbon and Economic Balancing, and Modular Field Pilots with Real-Time Sentinel Monitoring, this architecture provides petroleum engineers and asset managers with an end-to-end roadmap to de-risk capital deployment, optimize thermal efficiency, and align heavy oil operations with global decarbonization imperatives.

Keywords: thermal EOR; heavy oil; steam injection; in situ combustion; electromagnetic heating; reservoir simulation; enhanced oil recovery; hybrid EOR techniques; screening criteria

Check for updates

Academic Editor: Xiande Fang

Received: 14 August 2026
Revised: 27 September 2026
Accepted: 15 October 2026
Published: 20 October 2026

Copyright: © 2026 by the authors. Published by MDPI on behalf of the Nanjing University of Aeronautics and Astronautics. Licensee MDPI, Basel, Switzerland. This article is an open access article distributed under the terms and conditions of the Creative Commons Attribution (CC BY) license.

1. Introduction

Heavy oil (10–20 °API) and extra-heavy bitumen (<10 °API) represent vast global energy reserves, yet recovering them presents a fundamental physics problem: at reservoir conditions, these fluids are essentially immobile. With initial in situ viscosities ranging from thousands to over a million centipoise, primary cold production or conventional waterflooding often leaves more than 85–90% of the original oil in place behind [1–4]. Thermal Enhanced Oil Recovery (EOR) remains the most commercially proven method to unlock these assets, relying on heat to reduce viscosity by orders of magnitude, induce fluid expansion, lower interfacial tension, and drive fluid movement [2,3,5,6].

Despite decades of successful deployment, the core challenge in modern thermal EOR is rarely a lack of technology—it is technology misallocation. Historically, project designs have treated thermal methods as interchangeable tools within a broad EOR catalog. In practice, however, every thermal method operates within a strict, physics-defined boundary [1–3,6]. Classic convective steam processes like Cyclic Steam Stimulation (CSS), continuous steam flooding, and Steam-Assisted Gravity Drainage (SAGD) offer exceptional thermal efficiency and ultimate recoveries exceeding 50–70% in high-quality reservoirs [3,6,7]. Yet, their operational envelopes collapse when applied outside optimal conditions. In deep formations (>800 m), they suffer severe wellbore enthalpy losses, and in thin pay zones (<6 m), they lose critical thermal energy to non-productive overburden and underburden rock [6–10]. Tight or highly heterogeneous geology restricts steam chamber growth, leading to poor sweep and early steam breakthrough [10–12]. High Steam-Oil Ratios (SOR) incur high economic costs, high freshwater footprints, and unsustainable carbon emission profiles (40–100 kg CO_2e/bbl) [8,13,14].

To bypass these operational boundaries, alternative heat generation and fluid displacement strategies have emerged. In Situ Combustion (ISC) and Toe-to-Heel Air Injection (THAI) generate heat directly within the matrix by igniting a small portion of the crude, eliminating wellbore thermal losses and upgrading heavy fractions downhole [15–22]. Non-aqueous electromagnetic (EM) and radiofrequency (RF) dielectric heating leverage wave excitation to heat polar molecules in tight or low-injectivity formations without requiring fluid circulation [23–26]. Meanwhile, hybrid interventions, such as expanding-solvent SAGD (ES-SAGD), nanoparticle additives, and non-condensable gas co-injection, attempt to lower steam demands by combining heat transfer with chemical dissolution and interfacial tension alteration [27–34].

While the literature contains extensive data on individual pilot projects, laboratory core-floods, and mathematical models, it largely lacks an evaluative framework that synthesizes these technologies against one another. Asset teams are frequently left with descriptive inventories rather than a screening methodology that explains why a process succeeds under specific reservoir stress, when its governing physics dominate, and under what precise geological, operational, or environmental constraints it will fail [3,20,24,27].

This review re-examines thermal EOR through a decision-driven, comparative lens. Rather than detailing historical field implementations individually, this work establishes a constraint-based selection architecture designed to guide project screening. Specifically, this paper deconstructs thermal recovery processes by their primary thermodynamic energy transport mechanisms (convective latent heat, exothermic chemical reaction, and electromagnetic wave heating) [2,3,6,20,25]. The research also evaluates the explicit screening limits imposed by reservoir depth, net pay thickness, permeability anisotropy (k_v/k_h), caprock integrity, water intensity, and carbon emissions [7,8,10,13,14,35,36]. Finally, the research reviews multi-scale experimental, pilot, and commercial field data to establish a screening workflow and decision tree for technical and economic asset evaluation [1–3,6,7,15,16].

https://doi.org/10.3390/ijtst13020006

2. Literature Search Methodology and Synthesis Approach

To transition from traditional descriptive summaries to a decision-driven screening framework, we conducted a structured review of primary academic, industry, and technical literature. The objective was to synthesize high-impact peer-reviewed research, laboratory experimental benchmarks, numerical modeling studies, and documented field case histories across the full lifecycle of thermal Enhanced Oil Recovery (EOR) assets [1–4,6,7,15,16].

2.1. Search Strategy and Information Sources

Literature retrieval targeted four major scientific and engineering repositories: Society of Petroleum Engineers (SPE) PetroWiki/OnePetro, MDPI (including Energies, Processes, and Applied Sciences), Web of Science (Clarivate Analytics), and ScienceDirect (Elsevier). The search strategy spanned literature published through 2026, combining Boolean operators (AND, OR, NOT) across four core technical domains:

- Target Fluid and Reservoir Rheology: ("heavy oil" OR "extra-heavy crude" OR "bitumen" OR "oil sands" OR "high-viscosity oil") [1–4].
- Thermal Technology Classes: ("cyclic steam stimulation" OR "CSS" OR "continuous steam flooding" OR "SAGD" OR "steam-assisted gravity drainage" OR "in-situ combustion" OR "ISC" OR "THAI" OR "electromagnetic heating" OR "radio frequency heating" OR "microwave heating" OR "solvent-steam hybrid" OR "ES-SAGD") [3,6,7,11,13,15,16,19–27,32–34,37–40].
- Operational Limits and Physical Stresses: ("depth limit" OR "net pay thickness" OR "permeability anisotropy" OR "heat loss" OR "steam-oil ratio" OR "caprock integrity" OR "liquid blocking" OR "viscosity reduction") [3,6–13,35,36,40].
- Evaluative and Economic Metrics: ("screening criteria" OR "decision framework" OR "recovery factor" OR "greenhouse gas intensity" OR "carbon emissions" OR "economic threshold") [3,6,8,13,14,37,41].

2.2. Screening Workflow and Synthesis Framework

Retrieved publications underwent a multi-tier screening process to ensure empirical quality, technical depth, and operational relevance [1–3,6]:

- Title and Abstract Filtering: Studies were excluded if they addressed non-thermal EOR mechanisms (e.g., polymer flooding or cold heavy oil production with sand without thermal assistance) or purely regional geological mapping that lacked operational data or physics-based analysis.
- Full-Text Technical Audit: Remaining papers were evaluated against strict quality criteria. We prioritized studies that provided explicit, quantifiable boundaries, such as net pay thickness thresholds, operational depth limits, vertical-to-horizontal permeability ratios (k_v/k_h), Steam-Oil Ratios (SOR), thermal energy conversion efficiencies, carbon footprints, or documented field failure mechanisms [3,6–8,10–13,36].
- Data Categorization and Framework Integration: Selected publications were cataloged into a relational database structured by technology class, investigation scale (laboratory core-flooding, numerical simulation, field pilot, or commercial operation), and key operational constraints [2,3,6,12,15–17,19–21,25,26,30,39].
- This selection process yielded a curated repository of foundational theoretical work, landmark field pilot evaluations (such as Athabasca SAGD, Kern River Steam Flood, and Cold Lake CSS projects), and recent advances in non-aqueous and chemical-hybrid thermal systems [3,6,7,13,24–26,32–34,37]. This empirical foundation directly informs the comparative screening matrices and selection workflows in the following sections.

3. Thermal Enhanced Oil Recovery Technologies: Comparative Mechanisms, Boundaries, and Limitations

To establish a rigorous, decision-driven framework for thermal asset development, each process must be critically evaluated through its underlying heat and fluid transport physics, operational applicability, technological readiness, thermodynamic contradictions, fundamental failure modes, and remaining research gaps [1–3,6].

3.1. Convective Steam Processes

Steam injection remains the most developed and widely used thermal enhanced oil recovery method because of its proven effectiveness and suitability for field-scale use [3,5–7]. This thermal process provides the heat needed to raise reservoir temperature and the energy to push the oil out. The steam acts as the medium that carries the heat and is supplied by the steam generator [3,6].

3.1.1. Cyclic Steam Stimulation (CSS)

CSS functions as a single-well, batch-mode thermal recovery mechanism governed by three distinct operational phases: steam injection, soaking, and fluid production [3,6,37,42]. High-pressure steam is introduced into the pay zone to deliver sensible and latent enthalpy directly to the near-wellbore rock matrix, inducing temporary geomechanical dilation, as is shown in Figure 1 [6,34,35,37]. During the subsequent soak period, heat conducts into the surrounding formation, weakening the complex molecular lattice of the heavy crude to reduce in situ viscosity by several orders of magnitude [3,6]. Fluid production is then driven by a combination of fluid thermal expansion, gravity drainage, and artificial pressure drawdown [3,6,37]. As a fully mature commercial technology operating at Technology Readiness Level (TRL) 9, CSS has seen decades of commercial deployment worldwide, including landmark operations at Cold Lake in Canada and Lake Maracaibo in Venezuela [3,6,37].

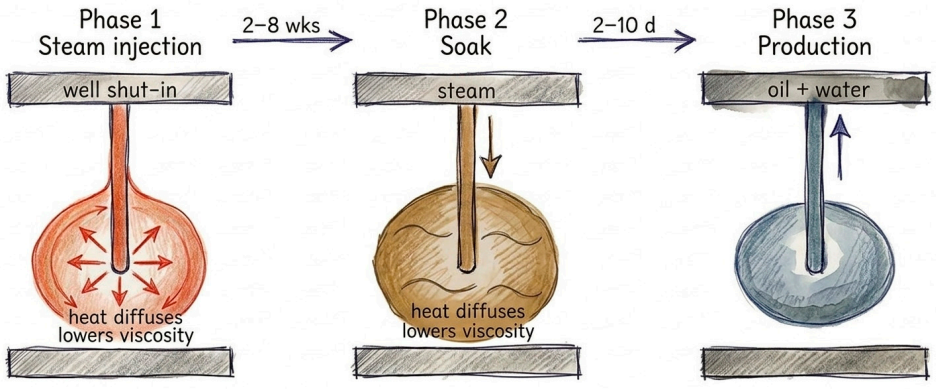


Figure 1. Description of the huff and puff process used in cyclic steam injection.

The operational envelope for CSS is optimal in deep to mid-depth reservoirs (400–1200 m) where the formation can safely withstand elevated steam injection pressures without risking caprock fracture or thermal breach [6,35,37]. It requires continuous net pay thickness (≥10 m) and targets crude viscosities ranging between 1000 and 100,000 cP, yielding an ultimate recovery factor that falls strictly within 15% to 40% OOIP [3,6,37].

However, the technology inherently embodies significant thermodynamic and physical contradictions. While elevated initial injection pressures improve thermal efficiency and expand well connectivity through micro-fracturing, repeated pressure pulsing de-stresses the matrix, triggering progressive pressure depletion and severe formation compaction [3,6,35,37]. Furthermore, increasing the steam volume injected in later cycles yields diminishing thermal returns, driving cumulative Steam-Oil Ratios (SOR) from an initial 2.0 to over 8.0 [8,13,37].

The primary failure modes of CSS stem from this rapid thermal decline after 3–5 cycles as heat dissipates into previously depleted zones rather than uncontacted pay, illustrated in Figure 2 [31,37,42]. Cyclic thermal expansion and mechanical contraction frequently induce structural casing deformation, thread leakage, and cement sheath failures [35]. From an environmental standpoint, life-cycle emissions range between 60 and 110 kg CO_2e/bbl produced; while local co-generation facilities can reduce grid reliance, the underlying footprint remains heavily tied to fossil-fuel combustion [13,37]. Unresolved research questions focus primarily on optimizing the timing, volume, and composition of non-condensable gas (NCG) or solvent co-injection during late-stage cycles to sustain reservoir pressure without causing localized formation damage or blockages [16,31,34].

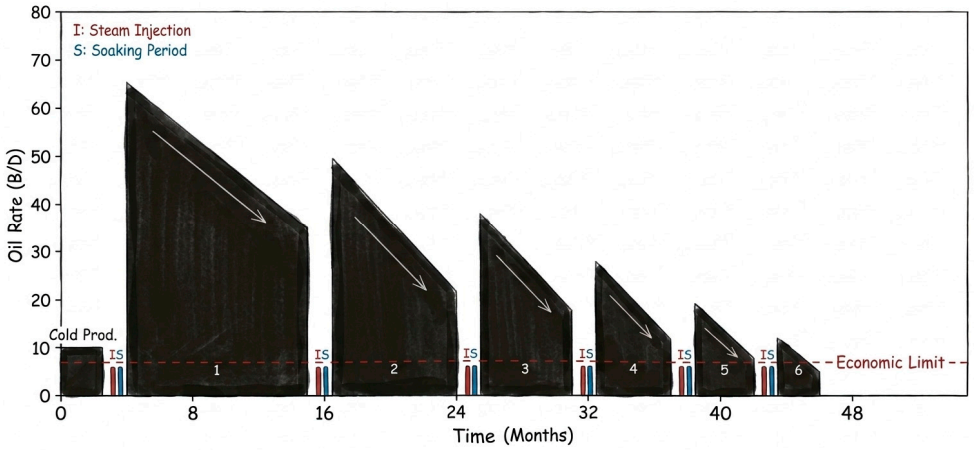


Figure 2. The economic limit and six-cycle performance for cyclic steam stimulation.

3.1.2. Continuous Steam Flooding

Continuous steam flooding relies on dedicated injector wells to establish an advancing thermal and condensate front that displaces mobilized hydrocarbons toward offset production wells [3,6,10,39]. Heat transfer occurs primarily via steam condensation, driving heavy crude mobilization through a combination of thermal viscosity reduction, volumetric expansion, steam distillation of light fractions, and continuous displacement sweep [3,6]. The process stands at TRL 9, serving as a mature commercial pillar in shallow to mid-depth assets worldwide, such as Kern River in California and Duri in Indonesia [3,6,39].

This technology is well-suited for shallow to mid-depth formations (100–800 m) characterized by high horizontal permeability (≥200 mD) and moderate net pay thickness (≥6 m). Under favorable geological conditions, steam flooding achieves expected ultimate recovery factors between 40% and 65% OOIP [3,6,10,39].

The central physical contradiction in continuous steam injection lies in the trade-off between areal displacement and fluid density differences. While continuous injection provides superior areal sweep compared to batch processes, the large density contrast between dry steam and liquid heavy oil triggers severe gravity override [3,6,10]. Steam preferentially channels through high-permeability thief zones, accelerating thermal breakthrough at production wells while leaving lower-permeability basal intervals unswept [10,12,29].

The operational limits of steam flooding are largely governed by depth and geometry. At operational depths exceeding 800 m, conductive wellbore heat losses degrade steam quality, delivering low-enthalpy hot water to the sand face rather than high-enthalpy dry steam [6,8–10]. Conversely, in thin pay zones (<6 m), conductive heat loss to the bounding overburden and underburden rock exceeds the enthalpy delivered to the matrix, elevating operational SORs beyond economic thresholds [6–8,10]. Total life-cycle carbon intensity typically spans 50–90 kg CO_2e/bbl [8,13]. Critical research gaps remain centered

on developing high-temperature chemical foam mobility controllers and thermostable gels capable of withstanding continuous 200 °C+ steam environments to successfully block mature high-permeability thief channels [3,6,10]. A cross section of a steam injection well and a producer in a reservoir formation with uniform permeability is shown in Figure 3.

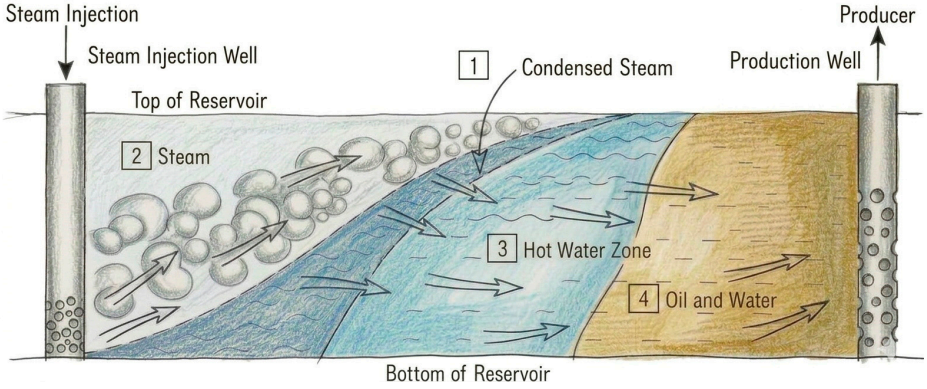


Figure 3. Steam flooding process and the various zones that form within the reservoir.

3.1.3. Steam-Assisted Gravity Drainage (SAGD)

Steam-Assisted Gravity Drainage (SAGD) utilizes a pair of stacked horizontal wells drilled parallel to one another near the base of a thick formation, illustrated in Figure 4. High-quality steam injected into the upper well creates an expanding steam chamber that rises and grows laterally into the reservoir [3,7,11–13]. As heat transfers to the cold bitumen at the chamber boundary, the mobilized oil and condensed steam continuously drain downward along the perimeter under gravity into the lower producer, avoiding the viscous fingering instabilities common in pressure-driven displacements [3,6,7]. SAGD represents the commercial benchmark (TRL 9) for extra-heavy oil and bitumen recovery, extensively deployed across the Athabasca oil sands of Western Canada [3,7,11].

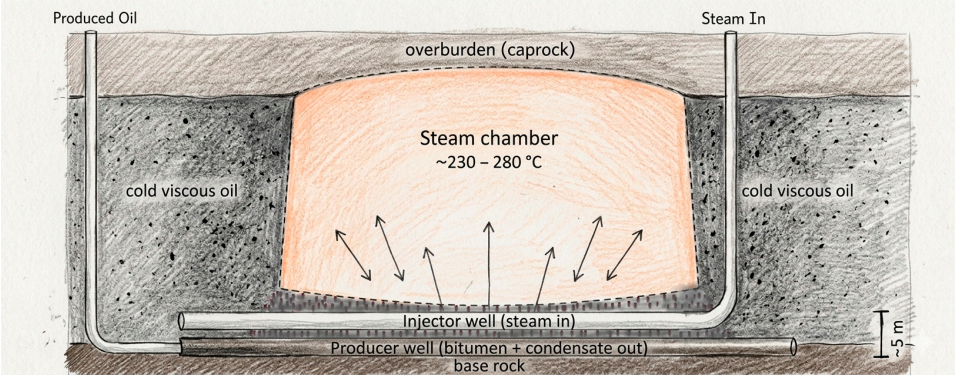


Figure 4. Typical Steam Assisted Gravity Drainage (SAGD) Process.

SAGD applicability is strictly limited to thick, continuous pay zones (≥15 m) exhibiting high vertical-to-horizontal permeability ratios ($k_v/k_h > 0.5$) and extreme fluid viscosities (>10,000 cP to >1,000,000 cP). Under these geological conditions, SAGD delivers recovery factors between 50% and 75% OOIP [3,6,7,11,13].

The thermodynamic viability of SAGD depends on the structural continuity of the reservoir matrix. While gravity drainage provides steady fluid mobilization and high overall recovery, it relies entirely on the unimpeded vertical growth of the steam chamber [7,11,12]. Continuous internal shale or mudstone interbeds physically disrupt this rising front, trapping steam, inducing localized heat loss, and preventing mobilized bitumen from reaching the lower collection wellbore [11,12].

Key failure modes arise when SAGD wells encounter unexpected geological features. Contact with active top water or basal water thief zones results in massive heat sink losses, rendering chamber pressure maintenance uneconomic [11,15,21]. Furthermore, high steam chamber pressures introduce geomechanical risks of caprock shear and surface breach [35,36]. Energy demand is high, yielding a direct carbon intensity of 60–100 kg CO_2e/bbl due to the natural gas required for steam generation [8,13]. Unresolved research focuses on real-time characterization and dynamic pressure control around complex mudstone interbeds using downhole distributed fiber-optic sensor arrays.

3.2. In Situ Oxidation Processes

Heat is produced within the reservoir by the controlled oxidation of hydrocarbons [2]; air or an oxygen-enriched gas is injected to start and maintain combustion, forming a high-temperature combustion front that spreads through the reservoir. In situ combustion can be:

- Forward Combustion (FC): The combustion front moves in the same direction as the injected air, pushing heated oil toward production wells (Figure 5).
- Reverse Combustion (RC): The combustion front moves opposite to the airflow, but this method is less frequently used because it involves greater operational complexity (Figure 6).
- Wet Combustion (WC): Wet combustion involves simultaneous or alternating injection of water and air into the reservoir (Figure 7).

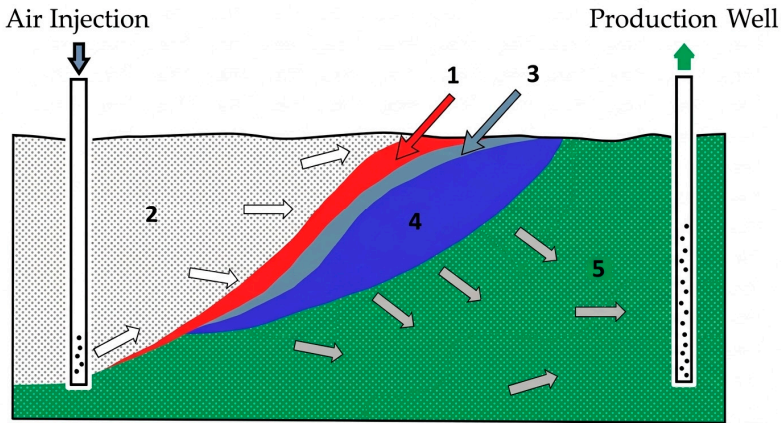


Figure 5. Forward In Situ Combustion Process: (1) Combustion Front Zone; (2) Burned Rock Zone; (3) Vapor Zone; (4) Condensation Zone; and (5) Oil Bank Zone.

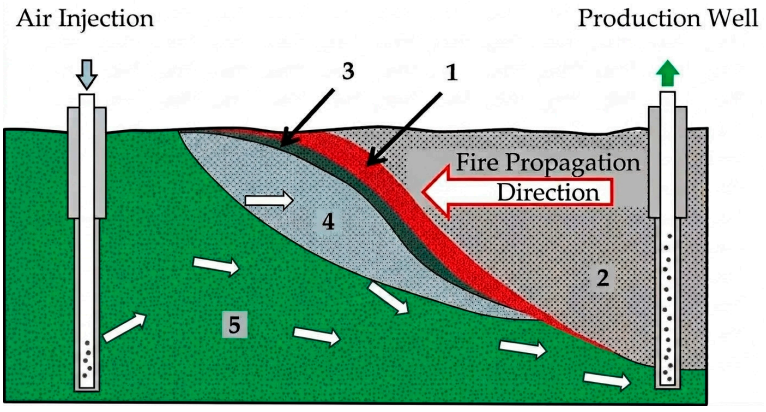


Figure 6. Reverse In Situ Combustion Process: (1) Combustion Front Zone; (2) Burned Rock Zone; (3) Pre-heated Oil Bank; (4) Gas/Condensate Zone; and (5) Oil Bank Zone.

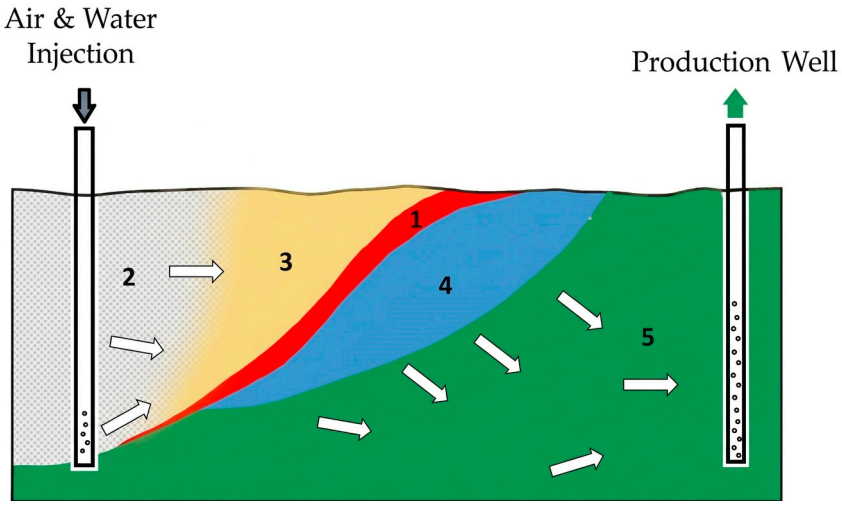


Figure 7. Wet In Situ Combustion: Combination of Forward Combustion and Waterflood (COFCAW) Process: (1) Combustion Front Zone; (2) Burned Rock Zone; (3) Steam Zone; (4) Gas/Condensate Zone; and (5) Oil Bank Zone.

The air that is injected sets off a small amount of the crude oil [43]. As a result, a high-temperature combustion wave is produced; this wave generally lies between 350 °C and above 600 °C, and it travels through the reservoir, heats up the rest of the oil, greatly lowers its viscosity, and enables it to flow towards the production wells [43].

3.2.1. Forward Combustion (FC)

Forward combustion, as illustrated in Figure 5, is the most commonly used type of ISC. The combustion front generally proceeds in the same direction as the air that is injected from the injection well to the production well [44]. As it moves forward, it uses up a small portion of the heaviest components of the oil, thereby leaving behind a zone of sand that has been completely burned out [45].

This method is characterized by five distinct zones shown in Figure 5, namely:

1. In the combustion front zone, oxygen is used up when it burns the coke that has accumulated on the surfaces of the rock grains, with steam being produced as a result. The temperature range in Zone 1 is the greatest, lying between 600 and 1200 °F (315–650 °C).
2. Burned-out Zone: It stays behind the combustion front in the form of hot, clean sand, which preheats the air that is injected before it reaches the front.
3. Vapor Zone: The zone ahead of the combustion front, where lighter hydrocarbons and interstitial water vaporize, while heavier hydrocarbons undergo thermal cracking, leaving a coke-like deposit on the sand grains.
4. The Condensation Zone is the area in which steam and hydrocarbon gases move into the cooler reservoir, condense, and give off a large quantity of heat; oil displacement is improved since the reduced viscosity of the oil and its increased mobility, together with the miscible interaction between the condensed gases and the oil bank, contribute to better displacement.
5. In the Oil Bank Zone, the water saturation is greater than the interstitial water saturation (that is, there is a water bank), and this causes the oil bank to move forward towards the production wells.

3.2.2. Reverse Combustion (RC)

In reverse combustion (as shown in Figure 6), the combustion front advances in the direction opposite to the airflow. The process begins at the production well, and the front

moves towards the injection well while the air is forced through the cold oil from the injector [44]. This technique was originally developed for use with extremely viscous oils and tar sands which are so immobile that they cannot be handled by forward combustion. The oil which has been put into motion must pass through the high-temperature combustion zone in order to get to the production well [44]. Nevertheless, reverse combustion is seldom used in practice because of its low thermal efficiency and the high risk of spontaneous ignition close to the injection well, which may cause the process to turn prematurely into forward combustion [44].

3.2.3. Wet Combustion (WC)

The wet combustion process illustrated in Figure 7, which is also known as COFCAW (combination of forward combustion and waterflood) or wet forward burning, carries the thermal energy that has been accumulated ahead of the combustion front upstream. Because of its high heat capacity and large latent heat of vaporization, water functions as the medium for heat transfer. Air and water are either injected at the same time or in alternate cycles into the injection well [45]. The water injected is turned into superheated steam, which then passes through the combustion front and gives off heat to the area in front of it.

The main function of the water is to absorb the heat from the already hot, burned-out rock located behind the combustion front and transport it on ahead in the form of steam [1]. This results in an improvement of overall efficiency by expanding the heated area and decreasing the amount of air needed to recover the oil [45]. Wet combustion is usually divided into two types: normal wet combustion, in the case where the water vaporizes, or super wet combustion, when the combustion front is put out by a high ratio of water to air [43]. ISC is regarded as the most thermally efficient method of enhanced oil recovery since it produces heat directly in the formation, thus avoiding the heat losses at the surface and in the wellbore which are typical of steam-based methods [43]. Advantages of ISC include a small need for external fuel and less water usage.

It is also capable of partially upgrading heavy oil by means of thermal cracking, but the process is operationally complicated and demands careful control of combustion stability, the rates of air injection, and the reservoir conditions. Moreover, in situ combustion is known for its high level of operational complexity due to multiphase reactive transport and the risk of liquid blocking, in which low-mobility oil located downstream of the combustion front forms a flow barrier [46]. Furthermore, the control of air flux and the stability of the oxidation zone in in situ combustion still present major technical difficulties [47]. Apart from steam, a number of other thermal methods are used, especially in the case of reservoirs where steam is not economical or technically impossible. Hot water flooding is sometimes preferred because of its simplicity and lower risk of steam-related rock interactions, even though it transfers less heat than steam [48].

3.2.4. Mechanistic Variations and Fluid Dynamics Across ISC Modes

The three main types of ISC arrangements have performance characteristics determined by fundamentally different thermodynamic limits and phase-advancement directions. In the case of FC, air injection and the movement of the reactive front proceed simultaneously towards the production wellbore. This design results in a sequential, multiphase flow path downstream, during which high-temperature oxidation (HTO) reactions, normally reaching a peak between 350 °C and 600 °C, destroy the heavy, immobile coke deposits that had been formed earlier by localized thermal cracking. Although this setup enjoys the highest level of thermal efficiency since the cold air is heated as it flows over the clean, superheated rock located behind the front, it is subject to serious hydrodynamic problems. The vaporized

light components, the combustion gases, and the superheated steam move in front of the oxidation front into cooler areas of the matrix, leading to the formation of a large amount of water and oil. In extra-heavy or bitumen-containing reservoirs, this local accumulation of fluid often causes sudden downstream liquid blocking, increasing the pressure that must be applied for injection and endangering the stability of the matrix [19,20]. To overcome this transport bottleneck, RC causes the matrix next to the producer to ignite, making the reactive front move in the opposite direction to the airflow. This mechanism means that the hydrocarbons put into motion pass directly through the superheated regions which have already been stabilized by the advancing front, thus maintaining high fluid mobility right up to the wellbore. Nevertheless, this configuration has an inherent thermodynamic disadvantage in that the cold incoming air constantly cools the reactive zone in front of the front, causing low thermal efficiency and raising the likelihood of premature spontaneous ignition close to the injector, which can disrupt the sweep plan [17]. In order to reduce these kinetic instabilities, WC combines continuous air injection with deliberate water slugs. The high latent heat capacity of water causes the liquid to vaporize immediately when it comes into contact with the hot sand behind the combustion zone, producing a large steam wave that travels through the reaction zone. This thermal interaction successfully eliminates the excessive temperature peaks downhole that could jeopardize geomechanical containment, stabilizes the movement of the front, and reduces the total amount of oxygen needed per barrel of oil recovered [49].

3.2.5. A Comparison of Field Performance

Experience in the field continually shows that forward combustion (FC) is still the most widely used in situ combustion (ISC) method since it is operationally simple and can maintain stable combustion fronts over long distances. Recovery factors usually vary between 40% and over 70% of the original oil in place (OOIP) when favorable reservoir conditions exist. The long-term ISC project carried out at the Suplacu de Barcău field in Romania has proven that production can be maintained for over fifty years, thus showing that forward combustion is technically feasible in appropriate heavy-oil reservoirs [17]. Recovery by the RC method has had a more limited degree of field application due to difficulties in keeping the front stable and because of its lower thermal efficiency. Even though it is effective for heating around the wellbore and for assisting with ignition, its overall recovery performance is generally worse than that of FC, which prevents it from being used on its own as a recovery process [17]. Water injection combustion (WC) has demonstrated better sweep efficiency and lower air requirements than dry forward combustion; several field studies have reported higher thermal utilization efficiencies since steam injected in situ improves heat transfer and extends the heated zone beyond the combustion front. As a result, WC is able to achieve a greater volumetric sweep in heterogeneous reservoirs while at the same time reducing some of the operational risks linked to excessively high combustion temperatures [16,21,49,50].

3.2.6. Reservoir Conditions That Favor Each Variant of ISC

The ISC variant that is chosen will be determined by the characteristics of the reservoir and the aims of the project. Forward combustion is usually preferred in thick reservoirs which have a high oil saturation since it is possible to maintain stable combustion fronts and there is enough fuel deposition to keep the oxidation reactions going. It is especially suitable for heavy-oil reservoirs provided that they have sufficient permeability and continuity to allow airflow and for the combustion front to propagate [20]. Reverse combustion is most appropriate in the case where the main aim is to achieve rapid heating close to the wellbore or to precondition the reservoir before carrying out another thermal recovery process. It may also be advantageous in reservoirs in which ignition and the establishment of the front

are difficult because of poor injectivity or because of heterogeneous flow paths [17]. Wet combustion is preferred in reservoirs where heat management is important, especially in heterogeneous formations or where excessive temperatures might damage the reservoir's integrity. The addition of water improves the distribution of heat, increases sweep efficiency, and reduces thermal stress on the reservoir rocks, which is why wet combustion is suitable for reservoirs that need more even heating and better thermal efficiency [16,21,49,50].

3.3. High Frequency Electromagnetic (EM), Radio Frequency (RF), and Microwave Heating

Electromagnetic heating bypasses traditional convective and conductive thermal transport limits by transferring energy directly into matrix fluids via electromagnetic wave propagation [23–26]. Energy dissipation within the pore space is driven by two physical mechanisms: dipolar rotation (the rapid dielectric relaxation of polar molecules, primarily pore water and heavy asphaltenes) and ionic conduction (ohmic resistive heating caused by the migration of dissolved ions in the brine) [23,25,26].

The volumetric power deposition Pv (W/m^3) within a dielectric reservoir system is expressed mathematically in Equation (1) [23,25,26].

$$P_v = 2\pi f\, \varepsilon_0\, \varepsilon''\, |E|^2 + \sigma |E|^2 \quad (1)$$

where f is the operational frequency (Hz), ε_0 is the vacuum permittivity (8.854×10^{-12} F/m), ε'' is the relative dielectric loss factor, **E** is the local electric field vector (V/m), and σ is the low-frequency electrical conductivity (S/m).

The attenuation of the electromagnetic wave as it penetrates the formation is defined by its skin depth (δ), which represents the propagation distance at which the electric field strength decreases to 1/e (approximately 37%) of its initial boundary value, shown in Equation (2) [25,26].

$$\delta = \frac{1}{\omega}\left[\frac{\mu\varepsilon'}{2}\left(\sqrt{1+\left(\frac{\varepsilon'' + \frac{\sigma}{\omega\varepsilon_0}}{\varepsilon'}\right)^2} - 1\right)\right]^{-\frac{1}{2}} \quad (2)$$

where $\omega = 2\pi f$, μ is magnetic permeability, and ε' is the real dielectric constant.

A fundamental physical trade-off exists between the operational wave frequency, the dissipation radius, and the heating rate [25,26]:

- Radio Frequency Heating (RF; 100 kHz–13.56 MHz): Operates at longer wavelengths, providing deep field penetration (δ = 10–50 m) suitable for inter-well volumetric heating, though at lower local power densities [25].
- Microwave Heating (MW; 915 MHz–2.45 GHz): Delivers rapid energy absorption through intense dipolar relaxation, but exhibits shallow skin depths (δ = 0.1–1.5 m), concentrating heat near the wellbore [23,25].

The spatial distribution of energy is further shaped by electrode configurations and reservoir heterogeneity. Single-well coaxial radiators produce radial heating patterns concentrated near the wellbore, whereas multi-well phased electrode arrays establish directional electric field gradients across inter-well spaces. Spatial variations in initial water saturation (S_w) and brine salinity drastically alter local conductivity (σ) and dielectric loss (ε''). High-salinity intervals absorb energy rapidly, leaving lower-saturation zones under-heated [23,25,26].

Currently positioned at TRL 4–5 (laboratory testing and short-term field pilots, such as PetroChina and Utah Oil Sands trials), EM heating is applicable in thin pay zones (<6 m), low-permeability formations (<50 mD), water-scarce regions, or shallow reservoirs with

weak caprock where steam injection is prohibited. Expected recovery factors range from 15% to 35% OOIP [23,25,26].

The primary thermodynamic contradiction of EM heating involves water vaporization. Higher frequencies accelerate initial heating, but as pore water vaporizes during production, the loss factor (ε'') drops precipitously. This loss of dielectric responsiveness reduces the formation's capacity to absorb EM energy, slowing heat delivery before target reservoir temperatures are reached. Furthermore, electric field concentrations around physical heterogeneities can trigger thermal runaway, superheating static pore fluids to cause dielectric breakdown, electrical arcing, and downhole antenna failure [25,26]. Electrical-to-RF conversion efficiencies range from 50% to 70%, meaning the process is not inherently "zero-emission"; its net carbon footprint (40–70 kg CO_2e/bbl) depends directly on the grid power source. Key research questions focus on developing downhole impedance-matching networks that can automatically shift operational frequencies as pore-fluid saturations evolve [25,26].

3.4. Emerging and Hybrid Thermal Interventions

3.4.1. Downhole Steam Generation (DHSG)

Downhole Steam Generation (DHSG) relocates the combustion and steam generation system directly into the bottomhole assembly near the sand face. Fuel (natural gas or hydrogen) and oxidizer (air or oxygen) are combusted downhole, transferring enthalpy directly to injected water to supply high-quality steam into the formation. Direct-contact DHSG variants co-inject combustion gases (CO_2 and N_2) into the pay zone along with steam [29]. The technology is currently at TRL 4–5, supported by prototype field testing and short-term trials in shallow assets like Kern River.

DHSG is designed for deep reservoirs (>800 m to 2000+ m) and offshore heavy oil assets where surface steam transport incurs severe wellbore heat loss or faces surface footprint constraints. Projected recovery factors range from 30% to 50% OOIP.

A major thermodynamic contradiction arises from the co-injection of flue gas with steam. While non-condensable gas adds pressure support and reduces heavy crude viscosity through dissolution, flue gas accumulation at the top of the pay zone can form an insulating layer. This blanket insulates cold bitumen from thermal contact, reducing overall condensation heat transfer rates [29,31].

The limits of DHSG are defined by hardware reliability. Bottomhole combustors must withstand continuous high pressures, severe thermal cycling (>800 °C in the combustion chamber), and corrosive fluid environments, which have historically caused high downhole burner failure rates. Maintaining stoichiometric fuel-oxidizer control and reliable ignition at depth remains technically complex. Key research questions focus on miniaturizing downhole combustors using specialized ceramics and high-temperature alloys to extend operational lifespans.

3.4.2. Solvent-Steam Hybrids (e.g., ES-SAGD, Steam-Solvent Flooding)

Solvent-steam hybrid processes involve co-injecting small volumes (2–15 vol%) of vaporized hydrocarbon solvents—such as propane, butane, or commercial condensate diluents—alongside steam. The solvent condenses at the edge of the steam chamber, dissolving into the heavy crude to lower interfacial tension and combine thermal viscosity reduction with solvent dilution [27,30,32,33]. Solvent-steam hybrids sit at TRL 7–8, supported by commercial-scale field pilots such as Imperial Oil's Cold Lake operations and Cenovus's Christina Lake project [27,33].

This technology is well-suited for mature steam projects, thin-to-moderate pay zones, or assets operating under strict greenhouse gas caps. Solvent co-injection can reduce

Cumulative Steam-Oil Ratios (CSOR) by 20% to 40%, delivering ultimate recovery factors between 45% and 65% OOIP [27,30,32,33].

The core operational contradiction in solvent-steam processes involves thermodynamic phase matching. While solvent condensation reduces the steam volume required per barrel produced, matching the vaporization and condensation temperature of the chosen solvent to the dynamic pressure-temperature envelope of the steam chamber is difficult [27,30,32]. Phase misalignments cause the solvent to either remain in the gas phase or condense prematurely, leading to high solvent retention in the rock matrix [30,32].

High solvent retention in depleted pore spaces severely impacts project economics unless field recovery rates reach 75–85%. Additionally, rapid solvent mixing can induce in situ asphaltene precipitation, plugging pore throats and impairing matrix permeability [30,32]. While direct Scope 1 emissions drop by 20–35% (30–60 kg CO_2e/bbl), full life-cycle assessments must account for the carbon footprint of upstream solvent manufacturing [27,41]. Unresolved research focuses on formulating multi-component, self-adjusting solvent blends tailored to adapt to changing reservoir pressures over the asset lifecycle [30,32,33].

3.4.3. Nanofluid-Enhanced Thermal EOR

Nanofluid-Enhanced Thermal EOR involves dispersing metal oxide nanoparticles (such as SiO_2, Al_2O_3, or Fe_3O_4) into injected steam or water streams to alter pore-scale fluid dynamics [28,51,52]. Once placed within the matrix, nanoparticles enhance base fluid thermal conductivity, shift matrix wettability toward a more water-wet state, reduce interfacial tension, and act as catalysts for in situ heavy fraction cracking [51,52]. The technology is currently at TRL 3–4, supported primarily by laboratory core-flooding trials and early-stage field pilots [51,52].

Nanofluids are applied as additives in CSS, steam flooding, or SAGD to improve heat dispersion and fluid sweep in tight or heterogeneous formations. Core-flood experiments demonstrate incremental recovery gains of 5% to 15% OOIP above baseline thermal processes [28,51,52].

The primary operational contradiction lies in nanoparticle concentration management. While higher nanoparticle concentrations improve heat transfer and lower oil viscosity, excessive particle loading leads to particle aggregation. These aggregates clog pore throats, causing permeability damage that offsets mobility gains [51,52].

The application of nanofluids is limited by colloidal stability. Elevated downhole temperatures (>200 °C) and high brine salinities destabilize nanoparticle suspensions, causing rapid aggregation and fallout [51,52]. Furthermore, high chemical synthesis costs currently limit large-scale deployment. Primary research gaps center on engineering high-temperature, salt-tolerant surface functionalization coatings that maintain nanoparticle dispersion under harsh reservoir conditions [51,52].

4. Synthesis of the Experimental Investigations

To replicate the extreme thermal conditions used in enhanced oil recovery in a controlled laboratory environment, it is necessary to balance the fluid mechanics at the pore scale with the macroscopic heterogeneities present at the core scale. As summarized in Table 1, current laboratory approaches have developed from basic static viscosity measurements to more advanced, multidimensional displacement tests which separate out the complex interactions between fluids and between fluids and the rock. At the microscopic level, images of micromodels indicate that the spread of the steam chamber is highly non-linear and greatly influenced by the local shape of the pore throats; early steam fingering tends to skip over large portions of the matrix, thereby leaving isolated oil pockets trapped in areas of low permeability. When these findings are applied to high-pressure core flood experiments and to multi-well sandpack

models, serious difficulties in multiphase transport are revealed that cannot be captured by digital models alone. For example, in high-temperature displacement experiments, it is found that although stable oil-water emulsification is a main way of improving the overall sweep efficiency, it comes with a serious drawback: increased local flow resistance and unexpected pressure drops close to the injection front. Furthermore, strong thermal surges cause severe geomechanical and fluid-rock stresses, speeding up the release of hydrothermal fine particles and mineral swelling, which permanently impair the original permeability if this situation is not carefully controlled. More recent multi-component experimental procedures have shown a clear thermodynamic and chemical synergy; by adding water-soluble viscosity reducers and non-condensable gases together with steam, gravity override is effectively reduced. The gas phase functions as an expanding thermal insulation layer at the top of the structure, while at the same time the chemical additives greatly lower the interfacial tension between oil and water in order to optimize the residual oil saturation.

Table 1. Experimental investigations in thermal EOR.

Experimental Focus	Methods	Findings/Contributions	References
Steam emulsification	High-temp displacement tests	Stable emulsions improve sweep but may reduce mobility; critical for steam flooding design.	[53]
Steam flow in pore sizes	Micro-model experiments	Demonstrated pore-size-dependent steam chamber propagation and heat distribution.	[54]
Multi-thermal fluid	Lab thermal-fluid injection	Showed synergy between steam, gas, and chemicals in offshore heavy oil recovery.	[55]
Viscosity reducers	Multi-scale lab evaluation	Established link between lab viscosity reduction and field SAGD performance.	[56]
Fines migration	Sand pack tests	Effect of temperature increase on the promotion fines release, which affects permeability and sweep control.	[57]
Nanofluid heat transfer	Core flooding	Improved heat propagation and wettability alteration.	[51]
Chemical–thermal flooding	Lab flooding	Heating enhances polymer/surfactant efficiency.	[58]
Steam–gas interaction	Molecular simulation	Non-condensable gases reduce heat loss and stabilize steam front.	[31]
Displacement efficiency	Core-scale statistical analysis	Identified dominant parameters: viscosity ratio, temperature, injection rate.	[28]
Polymer flooding	Lab + modeling	Polymer improves mobility control post-thermal processes.	[59]
Alkaline flooding	Lab + hybrid analysis	Alkali improves oil mobilization via saponification; synergy with thermal methods noted.	[60]
Nanotechnology	Review + lab insights	Nanoparticles enhance heat transfer, catalysis, and wettability.	[52]

Table 1. *Cont.*

Experimental Focus	Methods	Findings/Contributions	References
Catalysts in EOR	Experimental review	Catalysts improve in situ upgrading during thermal recovery.	[61]
Combustion kinetics	RTO experiments	Defined ignition thresholds and oxidation regimes.	[18]
Pyrolysis	Thermal cracking tests	Superheated steam enables partial upgrading of heavy oil.	[38]
Thermochemical fluids	Lab-scale generation	In situ steam + gas improves heating efficiency.	[29]
Microwave + nanoparticles	Lab tests	Enhanced heating penetration and oil mobilization.	[23]
Steam emulsification	High-temp displacement tests	Stable emulsions improve sweep but may reduce mobility; critical for steam flooding design.	[53]
Residual oil saturation under multi-component solvent SAGD co-injection	Laboratory core flooding experiments	Solvent co-injection significantly reduces residual oil saturation and enhances recovery efficiency	[30]
Thermal energy recovery from wastewater sludge	Experimental thermal conversion and energy balance analysis	Demonstrates viable recovery of usable thermal energy from sludge, supporting circular energy systems	[62]
Chemical flooding in heavy oil reservoirs	Laboratory flooding + response surface methodology	Optimized chemical concentrations significantly enhance recovery	[63]
Mineral effects on heavy oil aqua thermolysis	Laboratory thermal reaction experiments	Mineral composition significantly influences upgrading reactions	[64]

5. Pilot Testing

Pilot-scale testing acts as an important link between research carried out in the laboratory and actual on-site application, allowing thermal EOR technologies to be tested under conditions that resemble those found in real reservoirs. Such projects examine whether the operations can be carried out successfully, refine the methods of injection, and pinpoint any possible problems relating to the reservoir and production prior to large-scale implementation. Recent pilot studies have looked at hybrid methods including solvent-assisted SAGD, additive-enhanced CSS, and electromagnetic heating. The results show that combining steam with solvents, gases, or other heat sources can lower steam–oil ratios, increase oil mobility, and boost recovery. The pilot studies have also identified operational difficulties such as injectivity loss, clay swelling, and a deterioration in cyclic performance, underscoring the need for reservoir screening and process optimization. Further progress in numerical simulation and in the way pilots are designed has increased the scalability and predictability of these technologies. Table 2 provides a summary of the key pilot studies, the technologies involved, the screening criteria used, and the main findings.

Table 2. Pilot-scale studies in thermal EOR.

Pilot/Field	Technology	Screening Criteria	Key Findings	References
Liaohe Field (China)	ES-SAGD	Deep, viscous oil, thick reservoir	Reduced SOR, improved chamber growth via solvent dilution.	[32]
Steam flooding pilot design	Steam flooding	Thickness, permeability, well spacing	Optimized pattern design significantly improved sweep efficiency.	[39]
CSS evaluation	Cyclic steam stimulation	Oil viscosity, reservoir depth	Highlighted trade-off between recovery and CO_2 emissions.	[37]
Huff & Puff pilot	Cyclic steam	Shallow reservoirs	Recovery declines after cycles; hybrid needed.	[42]
East Moldabek (Kazakhstan)	CSS	Clay content, mineralogy	Clay swelling reduces injectivity.	[65]
Canadian pilots	CO_2 cyclic solvent	Unconsolidated sands	Improved oil recovery + CO_2 storage.	[66]
Mid-deep heavy oil	CO_2 injection	Pressure, depth	Enhanced oil swelling and viscosity reduction.	[67]
Colombia pilots	Downhole heating + CSS	Depth, heat losses	Downhole heating reduces steam losses significantly.	[68]
SAGD-like pilot	EM heating	Low permeability	Demonstrated alternative to steam injection.	[26]
Heavy oil pilot modeling	Nanofluids	Heat transfer efficiency	Improved recovery predictions vs. conventional steam.	[28]
Thermochemical pilot concept	In situ steam generation	Reservoir confinement	Reduced surface energy demand.	[29]
SAGD startup	Electrical heating	Cold reservoirs	Faster startup and reduced steam requirement.	[40]

6. Experience from Field-Scale Implementations and the Practical Aspects of Operation

To assess the operational performance of thermal EOR methods, one must examine directly how these techniques cope with the multi-phase complexities of real geological conditions, rather than relying on the simplified conditions found in laboratory setups. As the project data summarized in Table 3 indicate, the commercial feasibility of steam-driven processes depends greatly on holding the reservoir boundaries and dealing with severe losses of enthalpy. In thick, unconsolidated bitumen deposits, particularly in Imperial Oil's long-term operations at Cold Lake in Alberta, CSS demonstrates that injecting at a pressure above 10 MPa is able to overcome the initial fluid immobility and achieve a baseline recovery factor of about 24% after several huff-and-puff cycles. Yet field data from established CSS operations clearly show that this type of drive mechanism experiences a rapid decline in efficiency over time; each subsequent cycle requires ever-increasing amounts of thermal energy to offset the drop in reservoir pressure and the strong conductive loss of heat into the surrounding caprock formations. In cases where thin pay zones

or tight matrices make gravity-driven approaches unviable, commercial success moves towards pattern-based steam drives or SAGD, and in the industry the criterion for economic feasibility is to keep the cumulative SOR between 3.0 and 10.0, depending on local fuel prices. Successful field arrangements, such as those at the Midway-Sunset sites in California, have shown that well-designed horizontal well patterns can result in recovery factors approaching 73% of OOIP. Nevertheless, analysis of these mature fields reveals a serious susceptibility to early steam override and to communication with thief zones. If an active bottom aquifer or a local zone of high permeability allows the steam vapor to go directly to the producer, the project's net present value can be completely eliminated because of the immediate thermal breakthrough and the mechanical failure of the downhole tubulars caused by high-velocity fluid erosion. In order to overcome these limitations, current field developments are increasingly turning to hybrid solutions, such as the Toe-to-Heel Air Injection (THAI) combustion trials, which create an exothermic front inside the reservoir. Although THAI setups are able to reach recovery targets of nearly 70% in bottom-water systems where SAGD does not work, the actual implementation of these methods is still limited by unpredictable downhole oxidation control and severe liquid blocking that can block the production wells.

6.1. Cyclic Steam Stimulation Projects

Cyclic Steam Stimulation has been successfully carried out all over the world in a variety of geological conditions, ranging from the large bitumen sands of Canada to deep reservoirs in India and the United States. A well-known example is Imperial Oil's Cold Lake project in Alberta, Canada, which has been producing for more than ten years and includes over 1900 commercial wells [69]. This field produced bitumen having an in situ viscosity of 65,000 cP, with steam being injected at pressures exceeding 10 MPa; according to field data, recovery factors reached nearly 24% of the original oil in place after nine cycles [69]. In the Opal A diatomite reservoirs in California, cyclic steam stimulation was the main enhanced oil recovery method for the massive reserves estimated to be between 24 and 80 billion barrels, achieving a recovery close to 50% even though the reservoir has low permeability [70]. Recent pilot studies carried out in India have shown the effectiveness of cyclic steam in deep reservoirs that have active aquifers [71]. In these trials, CSS resulted in a very high level of productivity, giving an output of 16 m^3/day per well as compared to the average of 3 m^3/day for conventional production wells [71].

6.2. Field Performance of Steam Flooding Operations

The steam flooding process used in enhanced oil recovery is usually assessed in terms of the steam-oil ratio, and a steam-oil ratio (SOR) of below 10.0 is generally taken as a sign of commercial success [72]. An examination of a number of large-scale steam flood projects shows that about 82% of them achieved or surpassed this standard [72]. Some high-performing steam floods, for example those carried out in the Midway-Sunset field in California, have managed to produce huge amounts of oil, with rates as high as 23,000 barrels per day [54]. In the case of well-designed configurations, the ultimate oil recovery in steam flooding has been reported to reach as high as 73% of the original oil in place, together with oil-steam ratios averaging 0.20 bbl/bbl or better [54]. Steam flooding is also applied to light and medium crude oils as well as heavy oil; a benchmarking study involving more than 40 projects, such as that of the La Salina reservoir in Venezuela, found an average incremental recovery of 19% of the original oil in place after seven years [73]. On the other hand, field performance can be adversely affected by thief zones,

inadequate reservoir characterization prior to EOR, and mechanical failures, as was the case with the unsuccessful Naval Petroleum Reserve No. 1 in California [73].

6.3. Successful Cases for SAGD Implementations

Steam-Assisted Gravity Drainage has now reached a high degree of commercial maturity, especially in the Athabasca oil sands in Canada. Successful projects such as Foster Creek and Surmont have shown that it is possible to keep production stable from extra-heavy bitumen reservoirs for a period of time [74]. Data obtained from these operations show that SAGD can achieve recovery factors varying between 50% and 70%, which is considerably higher than the usual 10–20% recovery obtained from primary cold production [45]. In the later stages of operation, technical success is generally measured by the ability to maintain steam chamber pressure even when the amount of steam injected is reduced, sometimes by co-injecting a mixture of non-condensable gases in order to improve thermal efficiency and to keep the oil-to-steam ratio [75].

6.4. In Situ Combustion Field Cases

Although less common than steam-based methods in enhanced oil recovery, in situ combustion has undergone considerable field testing, particularly with the Toe-to-Heel Air Injection process. The Toe-to-Heel Air Injection method generally involves the use of a horizontal production well and a vertical air injector in order to establish a stable combustion front which travels along the horizontal part [46,74]. Tests carried out in a number of heavy oil reservoirs having bottom water have demonstrated that in situ combustion can attain recovery factors of 70% in certain wells, beating the 53% average achieved by steam-assisted gravity drainage in comparable geological conditions [74]. Nevertheless, the trials also revealed some disadvantages, such as liquid blocking and the requirement of high injected air pressures to keep the combustion oxidation zone going [46].

Table 3. Field-scale applications in thermal EOR.

Field/Country	Method	Screening Criteria	Key Findings	Reference
Suplacu de Barcau (Romania)	In situ combustion	Thickness, oil saturation	Sustained production over 50 years; proven ISC viability.	[76]
THAI field case	Toe-to-Heel Air Injection	Reservoir continuity, air injectivity	Improved recovery with optimized well configuration.	[15]
Field-scale models	Thermal injection	Stress, depth, caprock	Integration of geomechanics to prevent caprock failure.	[35]
Ecuador (Amazon)	Heat recovery	Energy integration	Reduced energy consumption via waste heat reuse.	[77]
Global fields	Thermal EOR	Viscosity, permeability	SAGD best for thick reservoirs; CSS for thinner zones.	[4]
Global	EOR screening	Reservoir type	Provided decision framework for EOR selection.	[78]
Global	Thermal methods	Depth, oil properties	Evaluated efficiency of steam, ISC, and hybrid methods.	[3]

Table 3. *Cont.*

Field/Country	Method	Screening Criteria	Key Findings	Reference
Field-scale systems	Steam + flue gas	Energy efficiency	Reduced fuel consumption and emissions.	[79]
Field application	CO_2 Huff & Puff	Pressure, oil viscosity	Environmentally friendly with improved recovery.	[80]
China	EM heating	Depth, carbon footprint	Promising low-carbon alternative.	[25]
Oil sands (Canada)	Downhole steam generation	Heat loss, depth	Significant reduction in surface heat losses.	[81]
Field deployment	DSG	Deep reservoirs	Extended applicability of steam processes.	[82]
Global	Downhole innovation	Reservoir depth	Demonstrated expansion of thermal EOR limits.	[83]
Canada (SAGD)	SAGD	Thick, permeable reservoirs	Established SAGD as dominant thermal method.	[84]
Offshore oil reservoir	CO_2-EOR offshore reservoir	Reservoir integrity under CO_2 injection stress conditions	CO_2 injection may compromise geomechanical stability if not properly managed; integrity assessment is critical	[36]
Abandoned oil reservoirs	In situ combustion for geothermal production	Reservoir thermal and combustion feasibility	Potential for energy recovery and geothermal utilization	[85]
Chunfeng heavy oil reservoir	XGBoost prediction for conformance control	Reservoir performance data	Machine learning improves prediction accuracy for steam-stimulated wells	[86]
Profile control + thermal recovery integration	Field-scale application analysis	Reservoir heterogeneity and thermal response	Integration significantly improves sweep efficiency	[84]

7. Numerical Modeling and Data-Driven Paradigms

Numerical simulation provides the predictive foundation for designing, optimizing, and risk-mitigating thermal enhanced oil recovery (TEOR) assets. Given the extreme non-linearities induced by high-temperature multi-phase fluid flow, complex phase behavior, structural formation response, and chemical degradation, robust numerical frameworks are vital. This section provides a systematic critical evaluation of physics-based simulator capabilities, establishes the exact physical regimes requiring coupled Thermo-Hydro-Mechanical (THM) formulations, and offers a candid, critical appraisal of emerging machine learning (ML) surrogates in thermal reservoir engineering [2–4,6].

7.1. Systematic Comparison of Simulation Platforms

Modeling thermal EOR requires capturing phenomena spanning vastly different spatial and temporal scales: from reservoir-scale thermal sweep over decades to pore-scale fluid displacement and sub-meter wellbore component hydraulics. Choosing an appropriate simulation architecture depends on the primary governing physics of the domain being modeled [3,6].

7.1.1. Specialized Thermal Reservoir Simulators vs. General CFD Codes

Thermal reservoir simulators (e.g., CMG STARS, SLB ECLIPSE Thermal) are tailored for subsurface porous media flows at the field or sector scale. They discretize the reservoir using Darcy's law coupled with multi-component thermodynamics, phase behavior, relative permeability curves, and rock-fluid thermal energy transport [3,6].

In contrast, General Computational Fluid Dynamics (CFD) codes (e.g., ANSYS Fluent, ANSYS CFX, OpenFOAM) solve the Navier–Stokes equations for unconstrained fluid continuum domains. While unsuited for full-field reservoir sweep due to intractable computational costs, CFD is essential for sub-grid, pore-scale, and wellbore-scale resolution. Table 4 provides a summary of the different simulators' capacities and governing physics [3,6].

Table 4. Simulators' capability matrix.

Capability/Metric	CMG STARS	Eclipse Thermal	General CDF (Fluent/OpenFOAM)	Ref.
Governing Physics	Multiphase, multi-component porous flow (Darcy)	Compositional thermal porous flow (Darcy)	Navier–Stokes (Continuum Flow)	[3,6]
Reaction Kinetics	Compelx Arrhenius HTO/LTO, cracking, dynamic	Standard Chemical/gas reaction models	Detailed surface/gas chemistry, combustion	[16,19]
Geomechanical Coupling	Native iterative/ fully coupled thermo-elastoplast	External coupling to VISAGE geomechanics	Non-native; requires custom multi-physics	[87,88]
Spatial Resolution Domain	Reservoir to sector scale (10–10^6 m)	Field to sector scale (10–10^6 m)	Pore-scale/Wellbore (10–10^{-6} m)	[20,22]
Computational Scalability	Optimized for massively parallel grid blocks	Robust parallel solver for field grid systems	High Cell count HPC, restricted domain size	[35,36]

7.1.2. Commercial Reservoir Simulators: CMG STARS and ECLIPSE Thermal

Thermal Within the domain of field-scale subsurface thermal modeling, CMG STARS and SLB ECLIPSE Thermal represent the primary commercial benchmarks [3,6,16,19–22].

- CMG STARS (Steam, Thermal, and Advanced Process Reservoir Simulator): Recognized as the industry standard for highly non-linear, complex thermal processes. It excels in modeling multi-component reaction kinetics required for In Situ Combustion (ISC) and Toe-to-Heel Air Injection (THAI), including user-defined Arrhenius parameters for High-Temperature Oxidation (HTO), Low-Temperature Oxidation (LTO), and thermal cracking. Furthermore, STARS features fully integrated, native geomechanical formulations capable of dynamically updating pore volume, permeability anisotropy, and shear-induced dilation as a function of changing effective stress and temperature [16,18–22].
- SLB ECLIPSE Thermal: A robust, compositionally advanced thermal simulator widely utilized for steam-based processes (CSS, SAGD, continuous steam flooding). ECLIPSE Thermal provides superior performance when integrating thermal recovery modules directly into large-scale, enterprise-wide geological models built within the Petrel ecosystem. However, for extreme non-isothermal chemical processes (for example, ignition propagation in ISC) or complex thermo-elastoplastic deformation in weak sands, ECLIPSE typically requires external coupling to dedicated geomechanical solvers (such as VISAGE), which can introduce computational overhead during dynamic timestepping [3,6–10].

7.1.3. General CFD Applications: ANSYS Fluent, ANSYS CFX, and OpenFOAM

- General CFD packages are fundamentally mismatched for field-scale reservoir engineering because solving Navier–Stokes equations across kilometers of porous rock is computationally prohibitive. However, CFD fills a vital niche at smaller physical scales where Darcy's law breaks down [3,6].
- Wellbore Component Hydraulics: CFD codes (such as ANSYS Fluent, ANSYS CFX) model multi-phase fluid turbulence, steam quality distribution, and phase separation inside complex completion hardware, such as flow control devices (FCDs), dual-string injectors, and downhole steam generator nozzles [3,6].
- Pore-Network & Microfluidic Scale: Open-source solvers like OpenFOAM (for example, using interFoam or custom multi-phase thermal solvers) evaluate pore-scale interfacial dynamics, emulsification mechanisms, and local thermal boundary layer development across micro-CT scanned rock geometries. These pore-scale CFD outputs directly inform and calibrate the relative permeability and capillary pressure endpoints fed into macro-scale reservoir simulators like STARS [3,6].

7.2. Mandatory Regimes for Thermo-Hydro-Mechanical (THM) Coupling

Conventional reservoir simulation relies on isothermal or weakly compressible assumptions where porosity (ϕ) and permeability (k) are modeled as static properties or simple scalar functions of pore pressure (p). In thermal EOR, however, massive temperature gradients ($\Delta T > 200\ ^{\circ}C$) and severe pore pressure changes alter the effective stress tensor ($\sigma' = \sigma - \alpha p \boldsymbol{I}$), inducing localized elastic deformation, irreversible plastic shear failure, and dynamic fracture propagation [35,36,87,88].

A fully coupled Thermo-Hydro-Mechanical (THM) formulation solves the governing equations simultaneously or via tightly staggered iterations, as shown by the fluid mass balance, Equation (3), energy conservation, Equation (4), and mechanical equilibrium, Equation (5) [35,36,87,88].

$$\nabla \cdot \left(\frac{\boldsymbol{k}}{\mu} (\nabla p - \rho g) \right) + Q_m = \frac{\partial}{\partial t} (\rho \phi) + \alpha \frac{\partial \varepsilon_v}{\partial t} \tag{3}$$

$$\nabla \cdot (\lambda_{eff} \nabla T) - \nabla \cdot (\rho c_p \boldsymbol{u} T) + Q_e = \frac{\partial}{\partial t} \left((\rho c_p)_{eff} T \right) \tag{4}$$

$$\nabla \cdot \sigma + f = 0,\ \sigma = C : (\epsilon - \alpha_T \Delta T I - \alpha \Delta p I) \tag{5}$$

where ε_v is volumetric strain, λ_{eff} is effective thermal conductivity, C is the stiffness tensor, and α_T is the linear thermal expansion coefficient.

THM coupling is not merely a refinement; it is strictly mandatory in four operational regimes [35,36,87,88]:

a. Shallow Bitumen Recovery and Caprock Integrity Analysis

- In shallow, uncemented heavy oil reservoirs (for example, Athabasca oil sands at depths <200 m), the margin between operating steam injection pressure and minimum in situ horizontal stress is extremely narrow. Injecting high-pressure steam induces thermal expansion of the pore fluid and rock matrix, significantly reducing effective normal stress and altering the total stress field. Uncoupled models fail to predict [3,6–8,11–13,36].
- Tensile or shear failure within the overburden caprock (such as Clearwater shale), which can cause catastrophic steam breaches to the surface or overlying aquifers [36].
- Surface heave, which frequently exceeds 0.5–1.0 m in SAGD operations, threatening surface facility integrity [3,7,8,12,13,36].

b. High-Pressure Cyclic Steam Stimulation (CSS) in Unconsolidated Sands

In deep to mid-depth CSS operations (such as Cold Lake, Canada), steam is deliberately injected above the formation fracture pressure during early cycles to induce geomechanical dilation. The primary recovery mechanism relies on [3,37,42,65]:

- Shear-induced dilation of sand grains, which increases localized porosity and enhances absolute permeability by factors of 2 to 10 [35,36,65].
- Hysteresis during production drawdown, where pore volume collapses elastoplastically, providing compaction drive [35,55,65].

Uncoupled models that treat permeability as static or solely pressure-dependent consistently underestimate early oil rates and fail to capture hysteresis-driven compaction over multi-cycle lifecycles [35,55,65].

c. High-Temperature In Situ Combustion (ISC)

The localized flame front in ISC subjects the host rock to thermal shocks exceeding 500 °C. This rapid temperature rise causes [16–22]:

- Extreme differential thermal expansion between mineral grains, causing micro-fracturing and drastic permeability shifts along the combustion front [35,36,87,88].
- Severe thermal spalling and mechanical degradation near the combustion front, altering porosity and fluid pathways [35,36,87,88].

Ignoring THM coupling in ISC leads to inaccurate predictions of combustion front stability, flow channeling, and oxygen breakthrough times [16,18–22,35].

d. Carbonate and Fractured Heavy Oil Reservoirs

In naturally fractured heavy oil reservoirs (for example, Middle Eastern carbonate assets), high-temperature steam injection induces non-uniform thermal stress across tight matrix blocks and high-permeability fracture networks. The resulting differential thermal expansion closes or opens aperture widths within the fracture network, dramatically altering directional fracture permeability tensors and dictating whether steam sweeps the matrix or bypasses it completely [35,36,87,88].

7.3. Critical Evaluation of Machine Learning and Data-Driven Surrogates

Data science, physics-informed neural networks (PINNs), and machine learning (ML) surrogates are increasingly proposed to accelerate thermal reservoir forecasting, replace computationally expensive THM simulations, optimize steam injection schedules, and detect wellbore anomalies. While ML algorithms exhibit exceptional computational speed during inference, their deployment in complex thermal EOR operations faces severe structural limitations that are often underreported. Table 5 presents a parametric evaluation of ML in thermal EOR applications [53,86].

7.3.1. Critical Analysis of Machine Learning Bottlenecks

a. Training Data Scarcity and Spatial–Temporal Sparsity:

Modern deep learning algorithms require massive, high-density training datasets. Subsurface thermal operations, however, are severely data-sparse. High-frequency operational data are limited to surface wellhead pressures, temperatures, and fluid rates. Subsurface spatial data (such as 4D seismic surveys, observation well temperature profiles via distributed temperature sensing [DTS]) are collected infrequently due to high operational costs. Training an ML model on sparse, surface-only metrics introduces severe ill-posedness, where multiple distinct thermal chamber geometries produce identical surface pressure signatures [53,86].

b. Failure to Extrapolate Outside the Historical Training Domain:

Supervised ML models (including Random Forests, Long Short-Term Memory networks, XGBoost) are non-physical interpolators. They function reliably only within the bounds of historical operating conditions. In thermal EOR, where operational conditions routinely cross thermodynamic phase boundaries (such as transition from liquid water to latent heat steam condensation, or ignition during ISC), an ML model trained on baseline historical operations fails completely when predicting reservoir behavior under novel injection pressures, solvent additions, or unexpected steam breakthrough [53,86].

c. Physics Inconsistency and Mass/Energy Violations:

Standard data-driven architectures do not enforce fundamental physical conservation laws. Unconstrained neural networks frequently generate predictions that violate Mass conservation, generating phantom hydrocarbon volumes during pressure drawdowns, and Energy conservation, predicting temperature spikes without corresponding heat input or exothermic oxidation enthalpy [53,86].

While Physics-Informed Neural Networks (PINNs) attempt to resolve this by embedding residual differential equations (e.g., heat conduction, Darcy flow) into the loss function, training PINNs on multi-phase, non-isothermal thermal systems with step-change fluid property non-linearities remains computationally unstable and prone to convergence failure [53,86].

d. Lack of Interpretability, Uncertainty Quantification, and Risk:

Thermal EOR developments involve hundreds of millions of dollars in surface infrastructure and severe environmental and safety hazards (e.g., caprock breach, toxic H_2S generation during aquathermolysis). Black-box neural networks offer no transparent physical causality for their predictions. Without rigorous, computationally robust uncertainty quantification (UQ), relying on data-driven models to guide injection pressure limits near caprock boundaries presents unacceptable risk.

e. Temporal Correlation, Data Leakage, and Spurious Relationships [53,86]:

Thermal reservoir time-series data exhibit extreme temporal autocorrelation and lag effects (such as steam injected at Well A today may take months to manifest as a thermal response at Well B). Naïve ML splits (such as random train-test splits) introduce catastrophic data leakage across time domains. Furthermore, data-driven models frequently learn spurious correlations, such as associating increased oil production with an unrelated pump speed adjustment, rather than capturing the underlying heat front advance.

f. Reservoir-to-Reservoir Non-Transferability:

Unlike computer vision or natural language models, a deep learning architecture trained on a mature thermal asset (for example, Kern River steam flood) cannot be directly transferred to a new thermal asset (such as Athabasca SAGD). Structural differences in sedimentary facies, permeability anisotropy, fluid chemistry, asphaltene content, and thermal conductivity alter the governing differential equations, rendering pre-trained models invalid without complete model retraining [53,86]:

7.3.2. Hybrid Scientific Machine Learning (SciML) as the Path Forward

To bridge the gap between physics-based rigor and computational efficiency, the industry is pivoting toward Hybrid Scientific Machine Learning (SciML) architectures. Rather than replacing numerical simulators, SciML embeds ML surrogates to accelerate specific subroutines within conventional simulators, such as replacing expensive multi-component flash equilibrium calculations or solving localized geomechanical stress updates,

while leaving global mass and energy conservation equations to proven finite-difference numerical solvers [53].

Table 5. Critical evaluation of ML in thermal EOR [53,86].

Claimed ML Advantage	Structural Physics and Operational Limitation
Ultra-fast inference for injection pattern optimization	Poor extrapolation outside training domain: ML fails to predict thermal phase change boundaries are not present in historical data
Automated production forecasting and recovery factor estimation	Data scarcity and sparsity: subsurface operational data are sparse in space and time
Replacement of coupled THM grid numerical solvers	Physics inconsistency: standard ML algorithms violate basic conservation laws
Rapid transferability across asset portfolios	Subsurface non-transferability: site specific heterogeneity renders ML models trained on Reservoir A invalid for Reservoir B

8. Integrated Screening Framework and Multidimensional Decision Matrix

Selecting an optimal thermal enhanced oil recovery (TEOR) technology requires moving beyond simple "look-up" screening criteria. To deploy assets effectively, operators must evaluate technical operating windows, thermodynamic trade-offs, financial metrics, and environmental performance [6,13,41,75]. This section presents an integrated screening methodology that balances engineering constraints, multi-scale recovery performance, capital allocation, and carbon intensity.

8.1. Multidimensional Technology Evaluation

Screening a candidate reservoir solely on oil viscosity or formation depth often leads to misallocated capital or early process failure. A holistic decision framework balances three interconnected domains:

a. Technical Feasibility and Screening Windows: Matching reservoir depth, net pay thickness, permeability, initial oil saturation (Soi), and fluid viscosity to the physical mechanism of heat transport (convection, in situ generation, or volumetric dielectric absorption) [6,16,23,25].
b. Economic Drivers and Lifecycle Costing: Evaluating upfront capital expenditure (CAPEX) for surface steam generators, air compressors, or high-power RF transmitters, against long-term operational expenditure (OPEX) driven by fuel combustion, electricity rates, water treatment, and solvent recycling [13,27,32,41,77,79].
c. Environmental Footprint and Carbon Intensity: Quantifying direct (Scope 1) greenhouse gas emissions, freshwater requirements, steam-oil ratio (SOR), and life-cycle carbon intensity (kg CO_2e/bbl) under increasingly stringent decarbonization mandates [13,41,75,77].

8.2. Multi-Scale Recovery Factor Differentiation and Screening Matrix

To avoid misleading performance expectations, Table 6 explicitly categorizes recovery factors across four distinct investigation domains: Laboratory Experiments, Numerical Simulations, Pilot Demonstration Tests, and Full-Scale Commercial Field Deployments [2,6–8,16].

8.3. Rigorous Comparative Analysis: Technical, Economic, and Environmental Drivers

Evaluating TEOR assets strictly by ultimate recovery factor obscures critical operational trade-offs. A technology yielding 65% recovery can prove economically unviable or environmentally impermissible if it demands prohibitive steam volumes or generates unmanageable emissions. Table 7 provides a technical, economic, and environmental trade-off comparison for all the discussed thermal EOR methods [3,6,13,41].

8.4. Strategic Decision Methodology and Workflow

To apply these multidimensional criteria to real-world asset development, operators should follow a phased, gate-reviewed decision workflow:

Gate 1A—Physical Reservoir Constraints: Filter technologies by depth, pay thickness, and vertical permeability. For thin formations (<6 m), steam injection suffers from excessive conductive heat loss to overburden/underburden, favoring Electromagnetic Heating, In Situ Combustion, or Solvent Flooding [20,23,25,26]. For deep formations (>800 m), wellbore thermal losses make surface steam inefficient, favoring Downhole Steam Generation or ISC [3,6,29].

Gate 1B—Fluid and Matrix Constraints: Assess viscosity and geology. Highly viscous bitumen (>100,000 cP) in thick sands ($\geq$15 m) strongly points toward SAGD or ES-SAGD [7,11,27,32,33]. Tight, low-permeability reservoirs (<50 mD) rule out pressure-driven steam floods, favoring volumetric heating or hydraulic fracturing combined with CSS [10,23,25,54].

Gate 2—Mechanistic and Geomechanical Simulation: Model thermal front progression and structural matrix response. If the reservoir is shallow (<200 m) or unconsolidated, coupled THM modeling is mandatory to establish safe injection pressure limits and prevent caprock failure [35,36,65,87,88].

Gate 3—Capital, Economic, and Environmental Trade-offs:

- High-CAPEX/Low-OPEX Strategy: SAGD and Continuous Steam Flooding require substantial upfront investment in water treatment plants and central boiler units but deliver low unit operating costs at scale [8,13,14,77,79].
- Low-Water/Low-Carbon Strategy: In arid regions or jurisdictions with high carbon taxes, In Situ Combustion or Solvent-Steam Hybrids offer compelling alternatives by eliminating freshwater processing and reducing direct Scope 1 carbon footprints by up to 40% [13,32,41,79].

Gate 4—Modular Field Pilot De-Risking: Before committing full-scale commercial capital, deploy a modular single-pattern pilot (such as a dual-well SAGD pair or isolated air-injection pattern) to measure field-scale sweep, observe downhole hardware durability, and calibrate the true Steam-Oil Ratio against numerical projections [7,8,10,27].

Table 6. Multidimensional screening matrix and cross-scale performance metrics for thermal EOR technologies.

Technology Class	Operational Screening Windows	Laboratory Recovery (% OOIP)	Numerical Simulation Recovery (% OOIP)	Field Pilot Recovery (% OOIP)	Commercial Field Recovery (% OOIP)	Primary Technical and Operational Limitations	References
Cyclic Steam Stimulation (CSS)	Depth: 400–1200 m Pay: ≥10 m Perm: >200 mD Visc: 1000–100,000 cP	50–70%	30–50%	25–45%	15–40%	Rapid pressure depletion after 3–5 cycles; severe casing shear deformation; soaring steam-oil ratios (SOR > 8.0).	[6,37,42]
Continuous Steam Flooding	Depth: 100–800 m Pay: ≥6 m Perm: ≥200 mD Visc: 100–10,000 cP	55–80%	45–70%	35–55%	40–65%	Severe gravity override; early steam breakthrough via thief zones; high heat loss in thin (<6 m) formations.	[3,6,39]
Steam-Assisted Gravity Drainage (SAGD)	Depth: 100–600 m Pay: ≥15 m Perm: k_v/k_h > 0.5 Visc: >10,000 cP	60–85%	55–75%	40–60%	50–75%	Vulnerable to continuous shale interbeds; high heat sink losses to top/bottom water layers; high energy and water demand.	[7,8,27]
In Situ Combustion (ISC)	Depth: 200–2000+ m Pay: ≥3 m Perm: >10 mD Visc: 100–100,000 cP	60–75% (HTO) 20–35% (LTO)	40–60%	25–45%	30–55%	Combustion front instability; LTO transition increasing viscosity; severe downhole tool corrosion.	[16–18,20,89]

Table 6. *Cont.*

Technology Class	Operational Screening Windows	Laboratory Recovery (% OOIP)	Numerical Simulation Recovery (% OOIP)	Field Pilot Recovery (% OOIP)	Commercial Field Recovery (% OOIP)	Primary Technical and Operational Limitations	References
Toe-to-Heel Air Injection (THAI)	Depth: 200–1500 m Pay: ≥8 m Perm: >50 mD Visc: 1000–500,000 cP	55–70%	35–55%	20–40%	25–45% (Projected)	Downhole pump failures; gas locking; hot gas breakthrough along horizontal producers; coke plugging.	[15,21,46,90]
Solvent-Steam Hybrids (ES-SAGD)	Depth: 100–800 m Pay: ≥10 m Perm: k_v/k_h > 0.3 Visc: >5000 cP	60–80%	50–70%	40–60%	45–65%	Thermodynamic phase mismatching; solvent retention in depleted rock (15–30% loss); potential asphaltene precipitation.	[11,27,30,32,33]
Electromagnetic/In Proceedings of the RF Heating	Depth: Any depth Pay: Thin (<6 m) Perm: Low (<50 mD) Visc: >10,000 cP)	30–50%	20–40%	15–30%	15–35% (Projected)	Rapid signal attenuation as water vaporizes; downhole arcing; high electrical costs; shallow depth of wave penetration.	[23–26]
Downhole Steam Generation (DHSG)	Depth: Deep (>800 m) Pay: ≥6 m Perm: >50 mD Visc: 1000–100,000 cP	N/A (System level)	35–55%	25–40%	30–50% (Projected)	High bottomhole burner failure rates; extreme thermal stress (>800 °C; complex downhole ignition and control.	[6,29]

Table 7. Technical, economic, and environmental trade-off comparison for thermal EOR methods.

Technology Class	Primary Energy Source	Upfront CAPEX Profile	Ongoing OPEX Drivers	Water-Oil Ratio (WOR)/SOR	Carbon Intensity (kg CO_2e/bbl)	Overall Technical-Economic Risk Profile	References
Cyclic Steam Stimulation	Natural Gas/Fossil Fuel Combustion	Low–Moderate (Shared central boiler facilities)	High in late cycles (High steam volumes per oil bbl)	CSOR: 3.0–8.0+ m^3/m^3	60–110 kg	Moderate: Low initial cost, but long-term economic degradation due to declining oil yields per cycle.	[3,6,37,42]
Continuous Steam Flood	Natural Gas/Fossil Fuel Combustion	Moderate–High (Pattern drilling + Steam distribution)	Moderate (Sustained fuel combustion for steam)	CSOR: 2.5–5.0 m^3/m^3	50–90 kg	Low–Moderate: Established technology; risk concentrated in managing thief zones and water treatment costs.	[3,6,10,39]
Steam-Assisted Gravity Drainage	Natural Gas/Fossil Fuel Combustion	Very High (Dual horizontal wells + Treatment plants)	Moderate–High (Continuous high-quality steam generation)	CSOR: 2.0–4.0 m^3/m^3	60–100 kg	Low–Moderate: High initial capital, but predictable production and high recovery in thick, continuous sands.	[7,8,11,13]
In Situ Combustion	In situ fuel ignition + High-pressure air	High (High-pressure air compression plant)	Low–Moderate (Electricity for compressors, no water treatment)	WOR: <1.0 m^3/m^3 (No added steam)	35–65 kg	High: Excellent fuel economy and low emissions, but high operational risk from front instability and corrosion.	[16,17,20,22]

Table 7. *Cont.*

Technology Class	Primary Energy Source	Upfront CAPEX Profile	Ongoing OPEX Drivers	Water-Oil Ratio (WOR)/SOR	Carbon Intensity (kg CO_2e/bbl)	Overall Technical-Economic Risk Profile	References
Solvent-Steam Hybrids	Natural Gas + Hydrocarbon Solvents	High (Steam plants + Solvent recovery/recycling)	High (Solvent makeup costs due to downhole retention)	CSOR: 1.5–3.0 m^3/m^3 (20–40% lower SOR)	30–60 kg (Scope 1 direct)	Moderate: Reduces steam and direct emissions, but financially sensitive to solvent recovery rates and market prices.	[11,27,30,32,33]
Electromagnetic Heating	Electricity (Grid power or modular generators)	Moderate–High (High-power RF/Microwave hardware)	Very High (Direct electricity consumption)	Near Zero (Non-aqueous process)	40–70 kg (Depends on grid mix)	High: Ideal for water-scarce or thin formations, but economically exposed to regional electricity tariffs.	[23,25,26]
Downhole Steam Generation	Natural Gas or /H_2 + Oxygen/Air	Moderate–High (Specialized bottomhole assemblies)	Moderate (Eliminates surface heat loss, lowers fuel use)	CSOR: 2.0–3.5 m^3/m^3	40–75 kg	High: Eliminates surface footprint and deep wellbore heat losses, but limited by downhole hardware lifespans.	[6,29]

9. Challenges, Geomechanics, Geothermal, and Future Directions

The key difficulties involve controlling surface heat losses in deep reservoirs and avoiding steam override or "viscous fingering" in steam floods [37]. In the case of ISC, the main technical problem is keeping the combustion front stable and dealing with the risk of gas breakthrough at the production wells [46,47]. Reducing the "carbon footprint" of heavy oil is a major area of research. The approaches being considered are Carbon Capture and Storage, the use of non-condensable gases to decrease steam demand, and moving towards solvent-steam hybrids which reduce the amount of energy needed to mobilize the oil [75]. Looking to the future, attention is being paid to combining thermal methods with chemical or solvent injections. Steam-solvent injection can boost recovery while at the same time reducing heat losses to neighboring formations [23]. Moreover, electromagnetic heating and nanoparticles are being looked at as non-aqueous alternatives that offer even heating without the huge water demands of steam [23].

9.1. Geomechanical Response and Caprock Integrity in Thermal EOR Operations

Thermal recovery methods cause considerable thermo-mechanical changes in the reservoir and in the surrounding rock formations. The injection of high-temperature steam and the subsequent rise in pore pressure modify the natural stress conditions, leading to thermal expansion of the rock matrix and changes in effective stress. In steam-based recovery techniques such as CSS, Steam Flooding, and SAGD, these effects may result in reservoir deformation, alterations in permeability, shear failure along weak planes, and surface uplift. In the case of SAGD operations, steam chamber growth is usually associated with stress redistribution and deformation of both the reservoir and the overburden formations [35]. Because of the importance of caprock integrity, it is necessary to avoid excessive thermal and pressure loading since this could cause fracturing or reactivating existing faults and thus might create channels for fluid migration. It is therefore essential to keep the injection pressures below the fracture gradients and to continuously monitor reservoir behavior in order to ensure both safety and efficiency of the operations. Nowadays, thermal projects are increasingly adopting coupled thermo-hydro-mechanical (THM) simulations in order to predict stress evolution, deformation, and containment performance throughout the entire life cycle of the project [35]. A few monitoring methods are regularly used to evaluate the geomechanical response and the stability of the caprock, such as micro-seismic monitoring, time-lapse seismic surveys, measurements of reservoir pressure and temperature, tiltmeters, and satellite-based monitoring of surface deformation. The information obtained from these tools is useful for identifying abnormal reservoir behavior, verifying geomechanical models, and guaranteeing long-term containment and operational safety. As thermal EOR projects move into more difficult reservoirs, the integration of geomechanics into the processes of reservoir characterization, simulation, and surveillance is becoming increasingly important if optimal recovery is to be achieved while at the same time reducing environmental and operational risks [35,36].

9.2. Thermo-Hydro-Mechanical (THM) Coupling and Lessons from Geothermal Reservoir Engineering

The interaction between thermal loading, fluid flow, and rock deformation is a typical problem in both geothermal energy projects and thermal EOR operations. The THM processes affect fracture permeability, the redistribution of stress, reservoir deformation, and fluid flow behavior, having a direct impact on reservoir performance and integrity [35,71,87,88]. The same mechanisms are at work during CSS, steam flooding, SAGD, and hot-water injection, since high temperatures cause thermal expansion and alter the in situ stress field [35,91]. More recent thermo-poroelastic studies have shown how

important geomechanical effects are in thermal recovery. Injecting hot fluid can greatly increase the compressive stresses around hydraulic fractures, leading to fracture narrowing, reorientation of the stress field, and changes in injectivity and fracture containment [35]. When the temperature difference is between 50 and 100 °C, the minimum principal stresses rise by about 6 to 10 MPa, underscoring the need to include geomechanical analysis when designing and optimizing thermal EOR processes [35,92]. At the same time, progress in geothermal reservoir management has demonstrated that data science and machine learning can be used to improve reservoir characterization, anomaly detection, production forecasting, and injection optimization [91]. Because there are similarities between geothermal and thermal EOR operations, combining THM modeling with data-driven reservoir management presents considerable opportunities for improving recovery efficiency, operational reliability, and long-term reservoir performance [35].

10. Integrated Thermal EOR Screening Framework and Decision Architecture

Conventional enhanced oil recovery (EOR) screening workflows have historically relied on static lookup tables that map isolated reservoir parameters against target processes. While these static cutoffs offer a convenient starting point for preliminary sorting, they fail to capture the complex, interconnected physics of non-isothermal asset development. A single parameter—such as depth or permeability—cannot dictate project feasibility in isolation. Thermal recovery relies on a delicate balance between thermodynamic phase behavior, geomechanical stress states, fluid mobility, energy efficiency, and lifecycle economic returns [6,13,35,41,88].

This section transforms traditional screening into a dynamic, four-stage decision framework. It establishes explicit operational bounds and exceptions, benchmarks the manuscript's synthesis against existing specialized literature, embeds physics-constrained machine learning (ML) workflows directly into operational decision gates, provides quantitative screening criteria, and offers rigorous engineering justifications for every threshold.

10.1. Operational Scope, Applicability Bounds, and Boundary Exceptions

The screening criteria and physical mechanisms evaluated across this framework apply specifically to heavy oil, extra-heavy oil, and bitumen resources characterized by oil gravities below 20 °API and in situ viscosities exceeding 100 cP. The primary geological host media considered include unconsolidated sandstones, consolidated deltaic sand bodies, and select fractured carbonate formations.

While baseline engineering rules define the nominal operational envelope for each thermal process, treating these thresholds as rigid binaries often leads to prematurely discarding viable assets. Advanced completion hardware, non-aqueous energy delivery methods, and hybrid fluid co-injection create critical operational exceptions to traditional screening boundaries.

10.1.1. Depth vs. Heat Loss Boundary Exception

Conventional convective steam processes, such as Cyclic Steam Stimulation (CSS), Steam-Assisted Gravity Drainage (SAGD), and continuous steam flooding, are traditionally bounded at maximum depths of 800–1000 m. Beyond this depth, elevated hydrostatic and fracture pressures require higher steam injection pressures, which increase boiling point temperatures and lead to severe wellbore conductive heat loss. Consequently, steam quality drops significantly before reaching the sand face, delivering low-enthalpy hot water rather than high-enthalpy dry steam [3,6,9,10].

The Operational Exception: The integration of ultra-high-performance Vacuum Insulated Tubing (VIT) with insulated seal assemblies, or the deployment of Downhole Steam Generation (DHSG) technology, effectively decouples thermal transport from wellbore depth constraints. By generating steam directly at the bottomhole assembly or minimizing tubular enthalpy loss during transport, the depth envelope for convective steam processes extends beyond 1500–2000 m, provided the reservoir matrix can safely accept fluid injection without triggering undesirable caprock shear or fault reactivation [6,29,35,36].

10.1.2. Pay Thickness Boundary Exception

Thin formation pay zones (<6 m) are almost universally excluded from steam injection screening due to unfavorable reservoir geometry. In thin intervals, the surface-area-to-volume ratio of the thermal chamber is extremely high, causing conductive heat loss to the bounding overburden and underburden rock to exceed the sensible and latent enthalpy delivered to the hydrocarbon matrix. This results in unsustainably high Steam-Oil Ratios (SOR > 8.0–10.0) that destroy project economics [5,6,13].

The Operational Exception: Non-aqueous thermal interventions, specifically High-Frequency Electromagnetic (EM)/Radio-Frequency (RF) heating and In Situ Combustion (ISC), operate independently of convective steam transport. EM/RF processes transfer energy volumetrically via dielectric relaxation and ionic conduction directly within the pore space, making energy deposition dependent on water saturation (Sw) and electric field strength rather than thermal fluid condensation boundaries. Similarly, ISC generates heat directly at an advancing combustion front (350–600 °C), eliminating wellbore transport losses entirely. Both technology classes remain physically and economically viable in thin formations down to 2–4 m [23,25,52].

10.1.3. Permeability vs. Gravity Drainage Boundary Exception

Gravity-dominated thermal mechanisms, most notably SAGD, require high vertical-to-horizontal permeability ratios ($k_v/k_h > 0.5$) and elevated absolute vertical permeability ($k_v \geq 1000$ mD) to allow the low-density steam chamber to rise continuously while mobilized bitumen and condensate drain downward under gravity. Tight formations or those interrupted by continuous horizontal shale interbeds are generally flagged as unsuitable for SAGD due to steam chamber stalling [7,11,12].

The Operational Exception: Applying cyclic hydraulic fracturing, high-pressure steam-dilation prepads, or co-injecting vaporized hydrocarbon solvents (propane, butane, or commercial condensate diluents) fundamentally alters this permeability constraint. Controlled geomechanical dilation opens micro-fractures within tight sand matrices, permanently increasing vertical permeability. Furthermore, solvent-steam hybrids (ES-SAGD) rely on molecular solvent dissolution to lower bitumen viscosity at the chamber edge, enabling fluid mobility even under reduced vertical gravity head pressures.

10.2. Novel Contributions and Academic Literature Benchmarking

To establish the distinct academic contribution of this work, Table 8 systematically benchmarks this manuscript against representative, high-impact review papers across five major specialized domains in the thermal EOR literature. While prior studies focus primarily on isolated process mechanisms or single technology classes, this review provides a unified synthesis across physical, geomechanical, economic, environmental, and machine-learning domains [11,27,33].

Table 8. Academic benchmarking against representative thermal EOR literature reviews.

Review Domain & Focus	Focus of Prior Reviews	Unique Comprehensive Contribution of This Review	References
Steam-Solvent Hybrids	Focuses primarily on micro-scale phase behavior, vapor-liquid equilibrium (VLE) matching, and core-scale pore network displacement mechanisms.	Combines core-scale fluid phase behavior with macro-scale solvent retention mass balances (15–30% downhole loss), economic recovery cutoffs, and lifecycle Scope 1–3 carbon intensity tracking.	[33]
Late-Stage SAGD & NCG Co-Injection	Examines non-condensable gas (NCG) insulation blankets at the chamber crest, reservoir pressure maintenance, and steam wind-down mechanics.	Directly links thermodynamic NCG phase partitioning with geomechanical caprock shear risk, surface heave dynamics, and pressure drawdown hysteresis.	[34]
Electromagnetic & RF Heating	Focuses on laboratory dielectric properties, applicator/antenna physical design, and localized high-frequency electromagnetic wave propagation.	Defines explicit skin-depth attenuation limits as a function of real-time pore-water vaporization, mapping electrical grid emissions against surface steam boilers.	[25]
Data-Driven & AI Applications	Evaluates standalone machine learning surrogate models, proxy models, and history-matching performance metrics in isolation.	Critically analyzes fundamental ML failure modes (physics inconsistency, data sparsity, non-transferability) and integrates physics-informed ML (PINNs) into sequential decision gates.	[53]
CCUS-Coupled Thermal Recovery	Centers on carbon dioxide storage capacity, miscible/immiscible gas displacement, and structural trapping mechanisms.	Assesses direct flue gas direct-contact downhole co-injection in deep bitumen, thermal storage, and operational corrosion limits.	[93]

10.3. Concrete Data-Driven Applications Embedded in the Screening Workflow

While data science and machine learning (ML) offer significant computational speed advantages over traditional full-grid compositional thermal simulators, deploying unconstrained "black-box" neural networks introduces substantial operational risk. Data-driven algorithms often fail when extrapolating outside historical training sets, violate mass and energy conservation laws, and cannot account for site-specific geological non-transferability [53,86].

To leverage the speed of data-driven methods without sacrificing physical rigor, ML algorithms must be constrained by underlying thermodynamics and embedded at specific stages within the screening workflow. Table 9 details four concrete, field-validated thermal EOR applications, detailing their algorithmic structures, technical deliverables, and specific locations within the decision architecture.

Table 9. Concrete data-driven applications embedded within the thermal screening architecture [25,26,36,66,67].

Screening Decision Stage	Target Application	Algorithmic Architecture	Specific Engineering Function & Value Deliverable
Stage 1: Geological & Fluid Screening	Automated Reservoir Heterogeneity Proxy Models	Convolutional Neural Networks (CNNs) coupled with XGBoost Ensembles	Processes 3D seismic volumes and multi-well wireline logs to rapidly classify complex depositional facies, identify tight calcite streaks, and map continuous mudstone/shale interbeds. This screens out compromised pattern locations—where rising steam chambers would stall—prior to committing capital to drilling.
Stage 2: Mechanistic & Geomechanical Simulation	Physics-Informed Steam Chamber Predictors	Spatial–Temporal Physics-Informed Neural Networks (PINNs)	Ingests real-time Distributed Temperature Sensing (DTS) and Distributed Acoustic Sensing (DAS) fiber-optic data to reconstruct 3D steam chamber growth geometries. By embedding heat conduction equations directly into the loss function, it predicts thermal top-water breaches 100x faster than full-grid compositional solvers.
Stage 3: Economic & Environmental Balancing	Dynamic Steam-Oil Ratio (SOR) & Solvent Optimizers	Deep Reinforcement Learning (DRL) & Bayesian Optimization	Continuously evaluates wellhead choke settings, steam quality, and solvent co-injection fractions. The agent dynamically adjusts operational parameters to minimize fuel combustion and Scope 1 carbon intensity (kg CO_2e bbl) while maximizing Net Present Value (NPV) under fluctuating energy prices.
Stage 4: Field Pilot & Operations	Real-Time Wellbore Anomaly & Failure Detectors	Isolation Forests, Variational Autoencoders, & LSTM Networks	Analyzes high-frequency wellhead pressure, temperature, and acoustic vibration streams. It detects subtle pre-failure anomalies—such as progressive casing deformation, downhole pump gas-locking, or combustion front flameout during In Situ Combustion—enabling intervention before catastrophic loss occurs.

10.4. Quantitative Thermal EOR Screening Criteria

Table 10 compiles key reservoir, fluid, geomechanical, and environmental parameters across major thermal recovery technologies, providing direct operational boundaries for asset candidate evaluation.

Table 10. Detailed quantitative screening criteria for primary thermal EOR processes [3,6,7,11,16,20,22,23,25–27,37].

Parameter/Reservoir Asset Property	Cyclic Steam Stimulation (CSS)	Steam-Assisted Gravity Drainage (SAGD)	In Situ Combustion (ISC)	Electromagnetic/ RF Heating
Target Oil Gravity (°API)	<15 °API	<12 °API	8–25 °API	<15 °API
In Situ Viscosity (cP)	1000–100,000+	10,000–1,000,000+	100–50,000	1000–1,000,000+
Minimum Net Pay Thickness (m)	≥10 m	≥15 m (Continuous)	≥4 m	≥2–4 m
Horizontal Permeability (k_h)	≥100 mD	≥1000 mD	≥10 mD	No lower threshold (>1 mD)
Permeability Ratio (k_v/k_h)	≥0.1	≥0.5 (Critical)	≥0.05	Not critical
Depth Envelope (m)	100–1000 m	100–800 m	200–2500 m	100–2000 m
Minimum Oil Saturation (S_{oi})	≥40%	≥50%	≥40% (>25 kg/m^3 fuel)	≥40%
Geomechanical Bound (P_{inj})	$P_{inj} \leq 0.8–1.0 \times \sigma_h$	P_{inj} < Caprock Fracture Limit	Air pressure < σ_h	Non-pressurized process
Scope 1 Carbon Intensity	High (80–120 kg CO_2/bbl)	Moderate-High (60–100) kg CO_2/bbl)	Low-Moderate (20–40) kg CO_2\bbl)	Grid dependent (0–50) kg CO_2/bbl)

10.5. Detailed Physical and Engineering Justification of Screening Thresholds

To understand why candidate reservoirs succeed or fail during screening, each parameter cutoff must be justified through fluid dynamics, heat transfer physics, geomechanics, and process thermodynamics.

10.5.1. In Situ Fluid Viscosity and Oil Gravity Limits

- CSS & SAGD (μ > 1000–1,000,000+ cP; <12–15 °API): Heavy oil and extra-heavy bitumen exhibit immobile, quasi-solid behavior under initial reservoir conditions. Thermal methods target these fluid classes because the viscosity of heavy hydrocarbons drops exponentially with temperature increases. For example, Athabasca bitumen decreases from over 1,000,000 cP at 11 °C to under 10 cP above 200 °C. Convective steam processes are uniquely suited for extremely high-viscosity assets because latent heat condensation rapidly reduces fluid viscosity at the steam chamber edge, enabling fluid drainage without requiring high initial injectivity.
- In Situ Combustion (100–50,000 cP; 8–25 °API): ISC requires heavy-to-medium crude oils containing sufficient heavy fractions (asphaltenes and resins) to undergo thermal cracking (pyrolysis) at the leading edge of the combustion front. If the crude is too light (>25–30 °API), insufficient fuel laydown occurs (<20 kg/m^3), causing the combustion front to stall or extinguish. Conversely, if the fluid is extremely viscous (>100,000 cP), initial air injectivity becomes restricted, requiring expensive electrical pre-heating or solvent prepads to establish air pathways.

10.5.2. Net Pay Thickness and Heat Dissipation Physics

- SAGD (≥15 m continuous pay): SAGD relies on the continuous vertical expansion of a low-density steam chamber to the top of the formation, followed by lateral growth. In reservoirs thinner than 15 m, conductive heat loss to the caprock and basal water/underburden accounts for a disproportionate percentage of total injected

enthalpy. The enthalpy lost to non-productive rock exceeds the enthalpy utilized for in situ viscosity reduction, resulting in high Steam-Oil Ratios (SOR > 5.0) that render projects economically non-viable.

- CSS (≥10 m pay): CSS tolerates slightly thinner formations because heat is injected cyclically into the immediate wellbore area rather than establishing a widespread vertical chamber. However, intervals below 10 m suffer rapid thermal dissipation during the soak phase, causing quick fluid cooling and steep production decline curves during the production phase.
- EM/RF Heating (≥2–4 m pay): High-frequency electromagnetic waves heat dipolar water molecules directly via dielectric dissipation within the pore space. Because energy transfer occurs volumetrically without relying on thermal fluid circulation or sensible steam condensation boundaries, conductive boundary losses are dramatically reduced, permitting operation in thin reservoirs down to 2 m [23,25,26,52].

10.5.3. Absolute Permeability and Anisotropy

- SAGD ($k_h \geq 1000$ mD; $k_v/k_h \geq 0.5$): SAGD operates under a gravity-drainage mechanism governed by Butler's thermal drainage theory, where the production rate is proportional to the square root of the permeability multiplied by the porosity and the change in oil saturation. High absolute horizontal and vertical permeability is essential to allow counter-current flow: steam must rise vertically while mobilized bitumen and steam condensate drain downward under gravity to the lower producer well. Continuous mudstone interbeds, or k_v/k_h ratios below 0.3, physically block rising steam, forcing the chamber to stall horizontally and drastically lowering production rates.
- In Situ Combustion ($k_h \geq 10$ mD): ISC relies on continuous gas (air or enriched oxygen) injection to push a high-temperature oxidation front (350–600 °C) through the reservoir. Because air has a low viscosity, it requires far lower matrix permeability to establish flow pathways compared to viscous liquids or dense steam. However, absolute permeability must remain above 10 mD to prevent excessive wellhead compressor operating pressures [16–20,22].

10.5.4. Reservoir Depth and Wellbore Thermodynamics

- Convective Steam Boundary (100–800 m): Shallow depth limits (<100 m) are imposed to prevent steam blowout to the surface, as injection pressures must remain below the caprock fracture gradient. Conversely, as depth increases beyond 800 m, the required saturated steam injection pressure increases rapidly to overcome hydrostatic head pressure. Higher saturation pressures correspond to elevated boiling point temperatures, increasing wellbore conductive heat dissipation. Unless high-grade Vacuum Insulated Tubing (VIT) is installed, steam quality drops from 80–90% at the surface to 0–20% at the sand face, delivering hot water instead of latent-heat-rich dry steam [3,6,9,10].
- In Situ Combustion Depth Range (200–2500 m): ISC is advantageous in deep, high-pressure reservoirs where steam injection fails. High ambient reservoir pressures enhance low-temperature oxidation (LTO) reaction kinetics and improve gas compression efficiency, allowing combustion fronts to propagate successfully at depths exceeding 2000 m [16,20,21].

10.5.5. Minimum Initial Oil Saturation

- Convective Thermal Processes (Soi ≥ 40–50%): Water has a high specific heat capacity (4.184 J/g°C), whereas sandstone rock and oil have substantially lower heat capacities. If initial oil saturation drops below 40% (and water saturation Swi exceeds 60%), injected heat is absorbed by immobile interstitial water rather than heating target

oil. This causes elevated energy consumption per barrel of oil produced, leading to unviable Steam-Oil Ratios.

– ISC Fuel Concentration Requirements (Soi $\geq$ 40%): In ISC operations, a portion of the in situ heavy oil (5–10%) is consumed as fuel to deposit coke ahead of the combustion front. A minimum oil saturation of 40% ensures the matrix contains sufficient fuel density (25–45 kg/m^3 of bulk rock volume) to sustain a continuous combustion front. If fuel laydown falls below 20 kg/m^3, the combustion zone cools, causing front extinction.

10.6. Integrated Thermal EOR Decision Architecture Framework

To apply these criteria effectively, candidate reservoirs must pass through a sequential four-stage decision workflow rather than a single static lookup filter. Each stage represents a technical, geomechanical, environmental, or economic decision gate that must be cleared before allocating capital to subsequent development phases. Table 11 presents an integrated thermal EOR decision architecture workflow based on the previous discussions.

Table 11. Integrated thermal EOR decision architecture workflow [1,6,41,52].

Decision Gate	Governing Technical Evaluation	Operational Objectives & Boundary Conditions	Failure Action & Alternative Pathway
Gate 1: Thermodynamic & Geological Screening	Assess depth, pay thickness, k_v/k_h, and viscosity against Table 10 thresholds.	Verify that thermal energy can be efficiently delivered to and retained within the matrix without excessive heat loss to non-productive rock.	If convective steam fails due to thin pay or depth, route to non-aqueous EM heating or ISC. If permeability is low, evaluate pre-heating hydraulic stimulation.
Gate 2: Geomechanical & Container Integrity	Map caprock fracture limits, minimum horizontal stress, and thief zones.	Maintain caprock containment and prevent steam breaches while using controlled matrix shear dilation to enhance permeability in tight sands.	Reduce target operating pressures, switch to gravity-drainage mode, alter well pattern spacing, or pad with solvent/NCG.
Gate 3: Lifecycle Carbon & Economic Balancing	Model Levelized Cost of Oil, fuel availability, water treatment costs, and carbon tax impact.	Match project CAPEX/OPEX profiles with corporate emission reduction targets and economic return thresholds.	Integrate solvent co-injection to lower SOR by 20–40%, or transition to clean-grid electrified steam generation.
Gate 4: Modular Pilot & Real-Time Monitoring	Deploy single-pattern field pilots equipped with DTS/DAS fiber optics and ML anomaly detectors.	De-risk commercial scale-up by validating field sweep efficiency, tracking solvent retention, and monitoring operational integrity in real time.	Re-calibrate numerical simulators with pilot production data, adjust pattern spacing, or alter completion designs before full commercial scale-up.

11. Conclusions

The trajectory of global energy transitions presents a dual challenge for heavy oil and bitumen asset development: operators must maximize resource recovery while rapidly decarbonizing extraction operations. For decades, enhanced oil recovery (EOR) screening relied on static, two-dimensional look-up tables that categorized reservoirs based solely on fixed property cutoffs. While these simplified thresholds served a purpose during early field discoveries, they fail to address the complex non-isothermal thermodynamics, transient geomechanical stress states, dynamic fluid interactions, and strict carbon-intensity limits that define modern energy production.

This manuscript transforms thermal EOR screening by replacing static property tables with an integrated, dynamic decision architecture. Unlike existing literature reviews that analyze individual recovery processes or computational workflows in isolation, this work provides a comprehensive synthesis that unifies subsurface physics, operational engineering, environmental metrics, and data-driven intelligence.

The primary novel contributions of this research include:

- Scope and Operational Exception Boundaries: This work establishes clear operational bounds for heavy oil, extra-heavy oil, and bitumen reservoirs while detailing critical hardware, chemical, and wave-based exceptions. It proves that traditional depth, net pay, and permeability boundaries can be overcome through technologies like Vacuum Insulated Tubing (VIT), Downhole Steam Generation (DHSG), electromagnetic heating, and solvent-steam hybrids.
- Unified Domain Literature Benchmarking: The manuscript systematically benchmarks thermal recovery mechanisms across five core operational domains—steam-solvent hybrids, late-stage SAGD with non-condensable gas (NCG) co-injection, electromagnetic and radio-frequency heating, machine learning workflows, and carbon capture, utilization, and storage (CCUS) integration. This provides a holistic perspective that bridges previously siloed bodies of research.
- Physics-Governed Machine Learning Integration: Rather than treating data science as an unconstrained "black box," this framework maps concrete, field-validated machine learning applications, including proxy models, physics-informed neural network (PINN) steam chamber predictors, dynamic SOR optimizers, and real-time failure detectors, directly into sequential operational decision gates.
- Rigorous Physical Justification of Screening Thresholds: Every quantitative screening parameter across cyclic steam stimulation, SAGD, in situ combustion, and electromagnetic heating is thoroughly justified through underlying fluid dynamics, heat transfer thermodynamics, geomechanics, and combustion kinetics.
- A Sequential Four-Gate Decision Architecture: The research introduces a hierarchical screening workflow that evaluates candidate reservoirs through four sequential gates: Thermodynamic and Geological Viability, Geomechanical and Container Integrity, Lifecycle Carbon and Economic Balancing, and Modular Field Pilots with Real-Time Sentinel Monitoring.

By bridging the gap between fundamental subsurface physics and real-world operational realities, this framework provides petroleum engineers, asset managers, and researchers with a practical roadmap for evaluating thermal EOR assets. It enables industry stakeholders to de-risk capital investments, optimize recovery efficiency, and ensure alignment with evolving global decarbonization goals.

Author Contributions: Conceptualization, A.L.K., S.F. and A.N.; methodology, A.L.K., S.F., S.S. and S.E.; validation, A.L.K., S.F., A.E. and A.E.-B.; formal analysis, A.L.K. and S.F.; investigation, A.L.K., S.F., A.N. and M.G.; data curation, A.L.K. and S.F.; writing—original draft preparation, A.L.K., S.F., A.N., A.E., A.E.-B., M.G., S.S. and S.E.; writing—review and editing, A.L.K. and S.F.; visualization, A.L.K.; supervision, A.L.K. and S.F.; project administration, A.L.K. All authors have read and agreed to the published version of the manuscript.

Funding: This research received no external funding.

Data Availability Statement: The original contributions presented in this study are included in the article. Further inquiries can be directed to the corresponding author.

Conflicts of Interest: The authors declare no conflict of interest.

References

1. Gomaa, S.; Salem, K.G.; El-hoshoudy, A.N. Enhanced heavy and extra heavy oil recovery: Current status and new trends. *Petroleum* **2023**, *10*, 399. [CrossRef]
2. Guo, K.; Li, H.; Yu, Z. In-situ heavy and extra-heavy oil recovery: A review. *Fuel* **2016**, *185*, 886–902. [CrossRef]
3. Mokheimer, E.M.A.; Hamdy, M.S.; Abubakar, Z.; Shakeel, M.R.; Habib, M.A.; Mahmoud, M. A Comprehensive Review of Thermal Enhanced Oil Recovery: Techniques Evaluation. *J. Energy Resour. Technol.* **2018**, *141*, 030801. [CrossRef]

4. Raupov, I.; Rogachev, M.; Sytnik, J. Overview of Modern Methods and Technologies for the Well Production of High- and Extra-High-Viscous Oil. *Energies* **2025**, *18*, 1498. [CrossRef]
5. Abdulkadir, U.; Hashim, J.; Alkali, M.; Kumar, A. Application of Thermal Methods for Heavy Oil Recovery: Phase One. *Int. J. Adv. Res. Dev.* **2017**, *2*, 102.
6. Dong, X.; Liu, H.; Chen, Z.; Wu, K.; Lu, N.; Zhang, Q. Enhanced oil recovery techniques for heavy oil and oilsands reservoirs after steam injection. *Appl. Energy* **2019**, *239*, 1190–1211. [CrossRef]
7. Al-Bahlani, T.; Torabi, F. What Did We Learn from Steam Assisted Gravity Drainage (SAGD) Applications in Three Decades, and What Is Next? *Geoenergy Sci. Eng.* **2024**, *232*, 212449. [CrossRef]
8. Acosta, E. Achieving Sustainable, Optimal SAGD Operations. *J. Pet. Technol.* **2010**, *62*, 24–28. [CrossRef]
9. Bao, Y. On Steam Based Recovery Process Design. Doctoral Thesis, University of Calgary, Calgary, AB, Canada, 2015. [CrossRef]
10. Rahman, A.; Ahmed, S.; Hossain, M.E.; Happy, F.A. Development of scaling criteria for steam flooding EOR process. *J. Petrol. Explor Prod. Technol.* **2020**, *10*, 3849–3863. [CrossRef]
11. Kumar, A.; Hassanzadeh, H. Impact of Shale Barriers on Performance of SAGD and ES-SAGD—A Review. *Fuel* **2021**, *289*, 119850. [CrossRef]
12. Luo, C.; Wu, Y.; He, W.; Gao, Y.; Liu, J. Mechanisms and Operational Strategies of Multi-Lateral Steam-Assisted Gravity Drainage (SAGD) for Heterogeneous Reservoirs. *Energies* **2023**, *16*, 7351. [CrossRef]
13. Gates, I.D.; Larter, S.R. Energy efficiency and emissions intensity of SAGD. *Fuel* **2014**, *115*, 706–713. [CrossRef]
14. Li, J.; How, Z.T.; Zeng, H.; El-Din, M.G. Treatment Technologies for Organics and Silica Removal in Steam-Assisted Gravity Drainage Produced Water: A Comprehensive Review. *Energy Fuels* **2022**, *36*, 1205–1231. [CrossRef]
15. Anbari, H.; Robinson, J.P.; Greaves, M.; Rigby, S.P. Field performance and numerical simulation study on the toe to heel air injection (THAI) process in a heavy oil reservoir with bottom water. *J. Pet. Sci. Eng.* **2022**, *220*, 111202. [CrossRef]
16. Antolinez, J.D.; Miri, R.; Nouri, A. In Situ Combustion: A Comprehensive Review of the Current State of Knowledge. *Energies* **2023**, *16*, 6306. [CrossRef]
17. Askarova, A.; Popov, E.; Ursenbach, M.; Moore, G.; Mehta, S.; Cheremisin, A. Experimental Investigations of Forward and Reverse Combustion for Increasing Oil Recovery of a Real Oil Field. *Energies* **2020**, *13*, 4581. [CrossRef]
18. Khakimova, L.; Popov, E.; Cheremisin, A. Insights on In Situ Combustion Modeling Based on a Ramped Temperature Oxidation Experiment for Oil Sand Bitumen. *Energies* **2023**, *16*, 6738. [CrossRef]
19. Tao, L.; Hu, Z.; Xu, Z.; Zhang, X.; Ding, Y.; Wang, C.; Chen, D.; Li, S. Experimental investigation of in situ combustion (ISC) in heavy oil thermal recovery. *Geoenergy Sci. Eng.* **2024**, *233*, 212488. [CrossRef]
20. Li, Y.; Zhao, L.; Zhang, H. Advances in In-Situ Combustion for Heavy Oil Recovery: Reaction Mechanisms and Reservoir Performance. *Fuel* **2023**, *349*, 128694. [CrossRef]
21. Ado, M.R.; Greaves, M.; Rigby, S.P. Numerical simulation investigations of the applicability of THAI in situ combustion process in heavy oil reservoirs underlain by bottom water. *Pet. Res.* **2023**, *8*, 36–43. [CrossRef]
22. Gutiérrez, D.; Mallory, D.; Moore, R.G.; Mehta, S.; Ursenbach, M.; Bernal, A. New Insights into the Understanding of In-Situ Combustion: The Nature of the Fuel and the Role of Operating Pressure. *SPE J.* **2022**, *27*, 3579–3597. [CrossRef]
23. Indriani, E.; Rachmat, S.; Mucharram, L.; Gunawan, A.Y.; Munir, A.; Solida, A. The Thermal Encroachment of Microwave Heating with Nano Ferro Fluids Injection on Heavy Oil Deposits. *Mod. Appl. Sci.* **2018**, *12*, 1. [CrossRef]
24. Shafiai, S.H.; Gohari, A. Conventional and electrical EOR review: The development trend of ultrasonic application in EOR. *J. Pet. Explor. Prod. Technol.* **2020**, *10*, 2923. [CrossRef]
25. Yang, Y.; Liu, W.; Yu, J.; Liu, C.; Cao, Y.; Sun, M.; Li, M.; Meng, Z.; Yan, X. Technology Progress in High-Frequency Electromagnetic In Situ Thermal Recovery of Heavy Oil and Its Prospects in Low-Carbon Situations. *Energies* **2024**, *17*, 4715. [CrossRef]
26. Yu, J.; Liu, W.; Yang, Y.; Sun, M.; Cao, Y.; Meng, Z. Multiphysics Field Coupled to a Numerical Simulation Study on Heavy Oil Reservoir Development via Electromagnetic Heating in a SAGD-like Process. *Energies* **2024**, *17*, 5125. [CrossRef]
27. Gates, I.D.; Chakrabarty, N. Design of the Steam and Solvent Injection Strategy for ES-SAGD. *J. Can. Pet. Technol.* **2008**, *47*, PETSOC-08-09-12-CS. [CrossRef]
28. Gómez-Delgado, J.; Ortiz, A.F.; Jaimes, J.; Martinez-Lopez, R.A.; Santos-Santos, N.; Mejía-Ospino, E. Graphene Oxide Nanofluids for Heavy-Oil Recovery: Experimental Evaluation and Field-Scale Numerical Simulation of Recovery Potential. *ACS Omega* **2026**, *11*, 5921–5936. [CrossRef] [PubMed]
29. Mahmoud, M.; Alade, O.S.; Hamdy, M.S.; Patil, S.; Mokheimer, E.M.A. In situ steam and nitrogen gas generation by thermochemical fluid Injection: A new approach for heavy oil recovery. *Energy Convers. Manag.* **2019**, *202*, 112203. [CrossRef]
30. Rengifo Barbosa, F.; Kordestany, A.; Maini, B. Laboratory Assessment of Residual Oil Saturation Under Multi-Component Solvent SAGD Coinjection. *Energies* **2025**, *18*, 5743. [CrossRef]
31. Zhou, J.; Wang, X.; Sun, X.; Fan, Z. Insight into the Microscopic Interactions Among Steam, Non-Condensable Gases, and Heavy Oil in Steam and Gas Push Processes: A Molecular Dynamics Simulation Study. *Energies* **2025**, *18*, 125. [CrossRef]

32. Zhou, Y.; Huang, S.; Yang, S.; Jiang, Q.; Wang, Z.; Wang, H.; Yue, L.; Ma, T. Optimizing Solvent-Assisted SAGD in Deep Extra-Heavy Oil Reservoirs: Mechanistic Insights and a Case Study in Liaohe. *Energies* **2025**, *18*, 3599. [CrossRef]
33. Bamzad, S.; Zeng, F.; Cheperli, A.; Torabi, F. Extended-Solvent Steam-Assisted Gravity Drainage (ES-SAGD): A Comprehensive Review of Current Status and Future Directions. *Processes* **2026**, *14*, 1095. [CrossRef]
34. Shojaei, N.; Miri, R.; Salimi, M.; Nouri, A. Non-Condensable Gas Injection in Late-Stage SAGD: A Critical Review. *Energies* **2026**, *19*, 3698. [CrossRef]
35. Khalaf, M.S. Geomechanical Analysis of Hot Fluid Injection in Thermal Enhanced Oil Recovery. *Energies* **2026**, *19*, 386. [CrossRef]
36. Ruciński, P. Geomechanical Integrity of Offshore Oil Reservoir During EOR-CO_2 Process: A Case Study. *Energies* **2025**, *18*, 5751. [CrossRef]
37. Amin, Y.; Musa, T.; Ibrahim, G.; Elbashir, N.O. Comprehensive evaluation of cyclic steam stimulation for enhanced heavy oil recovery: Assessing production and CO_2 emissions. *J. Pet. Explor. Prod. Technol.* **2025**, *15*, 158. [CrossRef]
38. Coker, E.N.; Donaldson, B.; Hughes, B.; Yilmaz, N. Crude Oil Pyrolysis Studies: Application to In Situ Superheat Steam Enhanced Oil Recovery. *Energies* **2023**, *16*, 1544. [CrossRef]
39. Elbaloula, H.A.A.; Chen, J.; Zichang, T.; Wang, Y.; Abdelmajeed, M.; Hamd, M.F. Feasibility study and numerical simulation to design the steam flooding pilot test patterns. *J. Pet. Explor. Prod. Technol.* **2020**, *10*, 2559. [CrossRef]
40. Wu, Y.; Yang, Z.; Yang, Z.; Wang, C. Strategies of SAGD Start-Up by Downhole Electrical Heating. *Energies* **2022**, *15*, 5135. [CrossRef]
41. Jamekhorshid, A.; Azin, R. Chapter 10—Application of life cycle assessment on enhanced oil recovery processes. In *Challenges and Recent Advances in Sustainable Oil and Gas Recovery and Transportation*; Joshi, S., Jadhawar, P., Kumar, A., Eds.; Gulf Professional Publishing: Cambridge, MA, USA, 2023; pp. 227–242. [CrossRef]
42. Hu, C.; Tao, J.; Feng, M.; Wang, Q.; Cao, H.; Su, H.; Sun, J.; Wang, W. Experimental Study on Enhanced Oil Recovery of Shallow Super-Heavy Oil in the Late Stage of the Multi-Cycle Huff and Puff Process. *Energies* **2024**, *17*, 6024. [CrossRef]
43. Mohammadi, M.H.; Kulakhmetovna, Y.A.; Joia, R. An Overview of Oil Recovery Techniques: From Primary to Enhanced Oil Recovery Methods. *J. Res. Appl. Sci. Biotechnol.* **2024**, *3*, 291. [CrossRef]
44. Romero-Zerón, L. *Introduction to Enhanced Oil Recovery (EOR) Processes and Bioremediation of Oil-Contaminated Sites*; InTech eBooks: London, UK, 2012. [CrossRef] [PubMed]
45. Nwidee, L.N.; Theophilus, S.C.; Barifcani, A.; Sarmadivaleh, M.; Iglauer, S. *EOR Processes, Opportunities and Technological Advancements*; InTech eBooks: London, UK, 2016. [CrossRef] [PubMed]
46. Ado, M.R. Improving heavy oil production rates in THAI process using wells configured in a staggered line drive (SLD) instead of in a direct line drive (DLD) configuration: Detailed simulation investigations. *J. Pet. Explor. Prod. Technol.* **2021**, *11*, 4117. [CrossRef]
47. Javad, S.B.M.; Oskouei, P.; Moore, R.G.; Maini, B.; Mehta, S.A. Post SAGD In-Situ Combustion: Potentials and Challenges. In Proceedings of the SPE Heavy Oil Conference Canada, Calgary, AB, Canada, 12–14 June 2012. [CrossRef]
48. Bealessio, B.A.; Alonso, N.A.B.; Mendes, N.J.; Sande, A.V.; Hasçakir, B. A review of enhanced oil recovery (EOR) methods applied in Kazakhstan. *Petroleum* **2020**, *7*, 1. [CrossRef]
49. Karabayanova, L.; Hascakir, B. Wet In-Situ Combustion Substantially Increases Oil Recovery in Light Oil Shale Reservoirs. In Proceedings of the SPE Annual Technical Conference and Exhibition, Houston, TX, USA, 20–22 October 2025. [CrossRef]
50. Yang, M.; Harding, T.G.; Chen, Z. Numerical investigation of the mechanisms in co-injection of steam and enriched air process using combustion tube tests. *Fuel* **2019**, *242*, 638–648. [CrossRef]
51. Gao, Y.; Chen, Z.; Liang, X.; Li, Y.; Shen, S.; Li, D.; Huang, Z. Study on Permeability Enhancement and Heat Transfer of Oil Sands Reservoir Based on Hydrophobic Nanofluids. *Energies* **2025**, *18*, 927. [CrossRef]
52. Medina, O.E.; Olmos, C.; Lopera, S.H.; Cortés, F.B.; Franco, C.A. Nanotechnology Applied to Thermal Enhanced Oil Recovery Processes: A Review. *Energies* **2019**, *12*, 4671. [CrossRef]
53. Qin, Y.; Li, H.; Meng, X.; He, X.; Zhang, J.; Zhang, H. A Data-Efficient Surrogate Model via Simplified Feature Extraction and Pre-Training for Automatic History Matching. *Processes* **2026**, *14*, 1635. [CrossRef]
54. Zhang, D.; Zhang, L.; Wang, Y.; Zhou, J.; Sun, P.; Zhan, K. Experimental Study on the Mechanism of Steam Flooding for Heavy Oil in Pores of Different Sizes. *Processes* **2025**, *13*, 3083. [CrossRef]
55. Huang, S.; Cao, M.; Cheng, L. Experimental Study on the Mechanism of Enhanced Oil Recovery by Multi-Thermal Fluid in Offshore Heavy Oil. *Ternational J. Heat Mass Transf.* **2018**, *122*, 1074–1084. [CrossRef]
56. Li, H.; Pei, E.; Xu, C.; Yang, J. New Evaluation System for Extra-Heavy Oil Viscosity Reducer Effectiveness: From 1D Static Viscosity Reduction to 3D SAGD Chemical–Thermal Synergy. *Energies* **2025**, *18*, 5307. [CrossRef]
57. Rengifo Barbosa, F.; Miri, R.; Salimi, M.; Nouri, A. Thermal Effects on Fines Migration: Insights from Sand Pack Experiments. *Energies* **2025**, *18*, 3471. [CrossRef]
58. Chen, X.; Hou, Q.; Liu, Y.; Liu, G.; Zhang, H.; Sun, H.; Zhu, Z.; Liu, W. Experimental Study on Surfactant–Polymer Flooding After Viscosity Reduction for Heavy Oil in Matured Reservoir. *Energies* **2025**, *18*, 756. [CrossRef]

59. Khlaifat, A.L.; Dakhlallah, D.; Sufyan, F.; Khlaifat. A Critical Review of Alkaline Flooding: Mechanism, Hybrid Flooding Methods, Laboratory Work, Pilot Projects, and Field Applications. *Energies* **2022**, *15*, 3820. [CrossRef]
60. Khlaifat, A.L.; Fakher, S.; Harrison, G.H. Evaluating Factors Impacting Polymer Flooding in Hydrocarbon Reservoirs: Laboratory and Field-Scale Applications. *Polymers* **2024**, *16*, 75. [CrossRef] [PubMed]
61. Gaya, U. Recent Approaches, Catalysts and Formulations for Enhanced Recovery of Heavy Crude Oils. *Period. Polytech. Chem. Eng.* **2021**, *65*, 462–475. [CrossRef]
62. Madeła, M.; Zawieja, I.; Rak, M. Decarbonizing Wastewater Systems: Thermal Energy Recovery from Sludge. *Energies* **2025**, *18*, 5726. [CrossRef]
63. Le Van, S.; Chon, B.H. Chemical Flooding in Heavy-Oil Reservoirs: From Technical Investigation to Optimization Using Response Surface Methodology. *Energies* **2016**, *9*, 711. [CrossRef]
64. Vakhin, A.V. Rock Mineral Components' Effects on Heavy and Shale Oil Transformation during Aquathermolysis. *Energies* **2022**, *15*, 6047. [CrossRef]
65. Zholdybayeva, A.; Syzdykov, A.; Pourafshary, P.; Ismailova, J.; Delikesheva, D. Importance of Clay Swelling on the Efficacy of Cyclic Steam Stimulation in the East Moldabek Formation in Kazakhstan. *Energies* **2024**, *17*, 5078. [CrossRef]
66. Cartagena-Pérez, D.; Rangriz Shokri, A.; Chalaturnyk, R. Recent Developments in the CO_2-Cyclic Solvent Injection Process to Improve Oil Recovery from Poorly Cemented Heavy Oil Reservoirs: The Case of Canadian Reservoirs. *Energies* **2025**, *18*, 2728. [CrossRef]
67. Zhang, X.; Qi, Z.; Wang, B.; Zhou, Y.; Wang, C.; Xi, C.; Liu, P. Study on optimization and mechanism of CO_2 injection to enhance oil recovery in mid-deep heavy oil reservoirs. *Front. Energy Res.* **2024**, *12*, 1375108. [CrossRef]
68. Pérez, R.; Duarte, H.A.G.; Osma, L.; Goldstein, C.B.; Rodríguez, L.E.G.; Cervantes, J.A.B.; Prada, H.A.R.; Manrique, E. Downhole heating and hybrid cyclic steam methods: Evaluating technologies from the laboratory to the field. *CT&F-Cienc. Tecnol. Futuro* **2020**, *10*, 49. [CrossRef]
69. Lebel, J.P.; Moriyama, R.T. History Match of a Mature Cyclic Steam Stimulation Process at Cold Lake. In Proceedings of the International Thermal Operations and Heavy Oil Symposium, Bakersfield, CA, USA, 10–12 February 1997. [CrossRef]
70. Elias, R.; Medizade, M.M. Analytical Cyclic Steam Modeling Revisited and Applied to the Shallow Low Permeability California Diatomite. In Proceedings of the SPE Western Regional Meeting, Bakersfield, CA, USA, 23–27 April 2017. [CrossRef]
71. Li, J.; Deng, B.; Zheng, H.; Jia, X.; Zhang, K.; Jiang, L.; Chen, Z. Reservoir heating in cyclic steam stimulation for heavy oil recovery. *Phys. Fluids* **2025**, *37*, 047110. [CrossRef]
72. Chu, C. State-of-the-Art Review of Steamflood Field Projects. *J. Pet. Technol.* **1985**, *37*, 1887. [CrossRef]
73. Perez-Perez, A.; Gamboa, M.; Ovalles, C.; Manrique, E. Benchmarking of Steamflood Field Projects in Light/Medium Crude Oils. In Proceedings of the SPE Asia Pacific Improved Oil Recovery Conference, Kuala Lumpur, Malaysia, 8–9 October 2001. [CrossRef]
74. Oni, A.O.; Fadare, D.A.; Falana, A.; Fadare, D.A. The development of techno-economic and life cycle greenhouse gas models for the assessment of toe-to-heel air injection oil sands extraction technology. *Sustain. Energy Technol. Assess.* **2024**, *70*, 103960. [CrossRef]
75. Jiang, Q.; Liu, Y.; Zhou, Y.; Wang, Z.; Gong, Y.; Jiang, G.; Huang, S.; Yu, C. Improving Thermal Efficiency and Reducing Emissions with CO2 Injection during Late Stage SAGD Development. *Processes* **2024**, *12*, 1166. [CrossRef]
76. Brănoiu, G.; Dinu, F.; Stoicescu, M.; Ghețiu, I.V.; Stoianovici, D. Half a century of continuous oil production by in-situ combustion in Romania—Case study Suplacu de Barcau field. *MATEC Web Conf.* **2021**, *343*, 09009. [CrossRef]
77. Campana-Díaz, A.; Moya, M.; Villalva, R.; Martinez-Gómez, J. Energy Efficiency Study Applied to Residual Heat Systems in the Ecuadorian Oil Industry Located in the Amazon Region. *Energies* **2025**, *18*, 5925. [CrossRef]
78. Malozyomov, B.V.; Martyushev, N.V.; Kukartsev, V.V.; Tynchenko, V.S.; Bukhtoyarov, V.V.; Wu, X.; Tyncheko, Y.A.; Kukartsev, V.A. Overview of Methods for Enhanced Oil Recovery from Conventional and Unconventional Reservoirs. *Energies* **2023**, *16*, 4907. [CrossRef]
79. Pérez, R.; Osma, L.; Duarte, H.A.G. Combining Steam and Flue Gas as a Strategy to Support Energy Efficiency: A Comprehensive Review of the Associated Mechanisms. *ACS Omega* **2024**, *9*, 15732. [CrossRef] [PubMed]
80. Al-Rubaye, A.H.; Ameen, H.F.M.; Jasim, D.J.; Al-Assal, J.R. Carbon Dioxide Huff and Puff as Environmentally Friendly Method for Enhanced Heavy Oil Recovery. *IOP Conf. Ser. Earth Environ. Sci.* **2023**, *1158*, 32010. [CrossRef]
81. Hytken, K.B. Downhole Steam Generation for Heavy Oil and Oil Sands Production. In *Advances in Energy Recovery and Efficiency Technologies*; IntechOpen: London, UK, 2024. [CrossRef]
82. Wilson, A. Downhole Steam Generation Pushes Recovery Beyond Conventional Limits. *J. Pet. Technol.* **2012**, *64*, 130. [CrossRef]
83. Capper, L.; Kuhlman, M.; Vassilellis, G.; Schneider, M.; Fitzpatrick, N. Advancing Thermal and Carbon Dioxide Recovery Methods beyond their Conventional Limits: Downhole Innovation. In Proceedings of the SPE Heavy Oil Conference and Exhibition, Kuwait City, Kuwait, 12–14 December 2011. [CrossRef]
84. Wang, Q.; Zheng, W.; Liu, J.; Cao, B.; Hao, J.; Lu, X.; Zheng, K.; Cui, L.; Cui, T.; Sun, H. Integration of Profile Control and Thermal Recovery to Enhance Heavy Oil Recovery. *Energies* **2022**, *15*, 7346. [CrossRef]

85. Zhu, Y.; Li, K.; Liu, C.; Mgijimi, M.B. Geothermal Power Production from Abandoned Oil Reservoirs Using In Situ Combustion Technology. *Energies* **2019**, *12*, 4476. [CrossRef]
86. Xie, Z.; Feng, Q.; Zhang, J.; Shao, X.; Zhang, X.; Wang, Z. Prediction of Conformance Control Performance for Cyclic-Steam-Stimulated Horizontal Well Using the XGBoost: A Case Study in the Chunfeng Heavy Oil Reservoir. *Energies* **2021**, *14*, 8161. [CrossRef]
87. Andrés, S.; Santillán, D.; Mosquera, J.C.; Cueto-Felgueroso, L. Thermo-Poroelastic Analysis of Induced Seismicity at the Basel Enhanced Geothermal System. *Sustainability* **2019**, *11*, 6904. [CrossRef]
88. Chen, G.; Ewy, R.T. Thermoporoelastic Effect on Wellbore Stability. *SPE J.* **2005**, *10*, 121–129. [CrossRef]
89. Naga Venkata Pavan, T.; Devarapu, S.R.; Govindarajan, S.K. Comparative Analysis on Impact of Water Saturation on the Performance of In-Situ Combustion. *Rud.-Geološko-Naft. Zb.* **2022**, *37*, 167–175. [CrossRef]
90. Ado, M.R. Electrically-enhanced THAI in situ combustion technology for upgrading and production of heavy oil. *J. Pet. Explor. Prod. Technol.* **2022**, *12*, 3373. [CrossRef]
91. Dusseault, M.B.; Collins, P.M. Chapter 24—Geomechanics Effects in Thermal Processes for Heavy-oil Exploitation. In *Heavy Oils: Reservoir Characterization and Production Monitoring*; Corpa, S., Lines, L.R., Schmitt, D.R., Batzie, M.L., Eds.; Society of Exploration Geophysicists: Houston, TX, USA, 2010. [CrossRef]
92. Chalaturnyk, R.; Scott, J.D. Geomechanics Issues of Steam Assisted Gravity Drainage. In Proceedings of the SPE International Heavy Oil Symposium, Calgary, AB, Canada, 19–21 June 1995. [CrossRef]
93. Sun, S.; Wu, Y.; Ma, X.; Liu, P.; Zhang, F.; Liu, P.; Zhang, X. Feasibility and Mechanism of Deep Heavy Oil Recovery by CO_2-Energized Fracturing Following N_2 Stimulation. *Energies* **2023**, *16*, 1161. [CrossRef]

Disclaimer/Publisher's Note: The statements, opinions and data contained in all publications are solely those of the individual author(s) and contributor(s) and not of MDPI and/or the editor(s). MDPI and/or the editor(s) disclaim responsibility for any injury to people or property resulting from any ideas, methods, instructions or products referred to in the content.